CHANGING PRIMARY PRODUCTION AND BIOMASS IN HETEROGENEOUS LANDSCAPES: ESTIMATION AND UNCERTAINTY BASED ON MULTI-SCALE REMOTE SENSING AND GIS DATA

by

Tingting Zhao

A dissertation submitted in partial fulfillment
of the requirements for the degree of
Doctor of Philosophy
(Natural Resources and Environment)
in The University of Michigan
2007

Doctoral Committee:

Professor Daniel G. Brown, Co-Chair
Adjunct Assistant Professor Kathleen M. Bergen, Co-Chair
Associate Professor David S. Ellsworth
Professor Christopher S. Ruf

To Mom and Dad

Acknowledgements

This work would not have been possible without the support from many people. I am especially indebted to my co-advisors, Dr. Daniel Brown and Dr. Kathleen Bergen, who have always been supportive of my doctoral education and research. Thanks also to my committee members, Dr. David Ellsworth and Dr. Christopher Ruf, who provided thoughtful questions and suggestions. I am grateful to Amy Burnicki and Dr. Herman Shugart, who prepared the land-cover data for the Michigan study and biomass quantities by forest categories for the Siberia study, respectively. Thanks to Shannon Brines, Derek Robinson, Jason Taylor, Dr. Geoffrey Duh, Qing Tian, Dr. Li An, Neil Carter, and Iryna Dronova, who have been great colleagues and friends. Thanks, finally but not least, to my husband, parents, and numerous friends, who always offer love and support.

This study was supported by the National Science Foundation Biocomplexity in the Environment grant BCS-0119804 and the NASA Land-Cover/Land-Use Change Program through contract NAG5-11084.

Table of Contents

Dedication ii
Acknowledgements iii
List of Tables vi
List of Figures viii
Abstract x
Chapter I Introduction 1
1.1 Productivity and biomass 4
1.2 Uncertainty of scale 5
References 8
Chapter II Increasing Productivity in Urbanizing Landscapes 10
Abstract 10
2.1 Introduction 11
2.2 Background 12
2.2.1 Characterizing development density 12
2.2.2 Evaluating primary production 13
2.3 Data and Methods 14
2.3.1 Study area 14
2.3.2 Land-cover data 15
2.3.3 Development density 16
2.3.4 Annual GPP 17
2.3.5 Changes in land cover and GPP by changes in development density 20
2.4 Results 21
2.5 Discussion 26
2.5.1 Increasing GPP in Southeastern Michigan 26
2.5.2 Uncertainties associated with land-cover data 29
2.5.3 Land-cover and GPP related to housing-unit density 32
2.6 Conclusions 33
References 35
Chapter III Census Scaling Effects on Inference of Productivity Trends 37
Abstract 37
3.1 Introduction 37
3.2 Study Area 39
3.3 Data and Methods 41
3.4 Results 45
3.4.1 Changes in development densities 45
3.4.2 Patterns of ΔGPP 47
3.5 Discussion 50
3.5.1 Scale dependence of housing and GPP inference 50
3.5.2 Mismatching census boundaries 52

3.6 Conclusions 54
References 55
Chapter IV Changes in Biomass at Landsat to AVHRR Resolutions 57
Abstract 57
4.1 Introduction 58
4.2 Study Area and Data 60
4.2.1 Study area 60
4.2.2 Data 61
4.3 Methods 62
4.3.1 Estimating biomass 62
4.3.2 Degrading spatial resolution 65
4.3.3 Analyzing scale dependence 66
4.3.4 Analyzing patch characteristics 68
4.4 Results 68
4.4.1 Changes in land cover and biomass at 60-meter resolution 68
4.4.2 Scaling effects 71
4.4.3 Spatial characteristics of the land-cover changes 77
4.5 Discussion 79
4.5.1 Changes in forest type and biomass due to land-cover change 80
4.5.2 Scaling and amplified estimates at MODIS/AVHRR resolutions 81
4.6 Conclusions 84
References 87
Chapter V Summary 90
5.1 ΔGPP in the U.S. developing region 94
5.2 Biomass trends in Eastern Siberia 96
References 98

List of Tables

Table 1.1 Comparison of the two study areas. 2

Table 2.1 Definition of land-cover types. 16

Table 2.2 Light-use efficiency (LUE, g C MJ^{-1}) used in the estimation of daily GPP by land-cover types. LUE of built-up was approximated from values of tree and crop/grass, which came from Turner *et al.* (2003) for case 1-5 and Running *et al.* (2000) for case 6. 20

Table 2.3 Area proportion (%) of the classified land-cover types in 1991 and 1999. 22

Table 2.4 Land-cover proportions and annual GPP (GPP_{gs}) by development-density categories in 1991 and 1999. Values in parentheses are standard error of mean. 22

Table 2.5 Changes in land-cover proportions and annual GPP (GPP_{gs}) between 1991 and 1999 by development-direction classes. 25

Table 3.1 Definition of development types 43

Table 3.2 Accuracy of categorization of development types (Kappa). Reference was the block-group level results. 47

Table 3.3 Spatial autocorrelation of changes in housing density across four Census scales. Changes in housing density were clustered at the block-group scale only. 48

Table 3.4 Spatial autocorrelation of the estimated ΔGPP across four Census scales. Significant autocorrelation was found at all scales. 48

Table 4.1 Biomass values assigned to individual land-cover classes 64

Table 4.2 Changes in land cover (%) and biomass (Mg C ha^{-1}) at the 60-meter resolution. The *subtotal* and *total* is the sum of Δbiomass weighted by proportions of area occupied by individual land-cover change types. 69

Table 4.3 Proportions of land-cover change types at 60- and 960-meter resolutions. Their differences in proportion with respect to their 60-m proportion are shown in bold numbers, where negative values indicate under-estimation of area at the 960-meter resolution and positive values over-estimation. 75

Table 4.4 Regression model results for the relationship between RMSE of the estimated Δbiomass at 960 meters and patch metrics of individual LCC types at 60 meters. The pixel-wise RMSE was pooled by LCC types at each case study site. In all three models, RMSE is the dependent variable. Independent variables include patch indices and site indicator. The adjusted R square is the indicator of model fit. 79

List of Figures

Figure 1.1 Changes in forest ecosystem gross primary production (GPP), net primary production (NPP), respiration (R) and biomass (B) after stand-initiating disturbances (adapted from Odum, 1969, Figure 1). 2

Figure 2.1 Study area covered ten Southeastern Michigan counties shown in thick black outlines, with the Detroit-Ann Arbor-Flint consolidated metropolitan statistical area displayed in white color. 14

Figure 2.2 Annual GPP (GPP_{gs} , g C m^{-2} $year^{-1}$) by development-density categories (a) and its changes by development-direction classes (b). Error bars in (a) indicated the maximum and minimum annual GPP, which were calculated using the highest and lowest light-use efficiency (LUE) of tree and crop/grass adapted from Turner *et al.* (2003). Error bars in (b) indicated the maximum and minimum changes in annual GPP, which were calculated from the cross-combination of the highest and lowest LUE for tree and crop/grass adapted from Turner *et al.* (2003). 24

Figure 2.3 The pixel-wise regional average of (a) biweekly AVHRR NDVI (adjusted to units of MODIS NDVI) and (b) estimated daily GPP (GPP_d , g C m^{-2} day^{-1}) over the growing season between early May and early October. Dates on the x-axis corresponded to the starting date of each bi-weekly time period in 1991. 27

Figure 3.4 Comparison of results using our land-cover classifications (1991 and 1999) with those using the NLCD (1992) and IFMAP (2000) classifications: (a) estimated annual GPP (GPP_{gs}), (b) land-cover proportions in 1991 and 1992, and (c) land-cover proportions in 1999 and 2000. 31

Figure 3.1 Study area included Detroit-Ann Arbor-Flint metropolitan (gray) and surrounding areas in ten Southeastern Michigan counties. 40

Figure 3.2 Development types and their distribution across the study area at the block-group (a), tract (b), county-subdivision (c), and county (d) levels. 45

Figure 3.3 Proportion of the total study area by development types at four Census scales. 46

Figure 3.4 The estimated ΔGPP by development types at four Census inference scales. Relationships between ΔGPP and development types were retained similar across all Census levels. The standard error of mean (s.e.m.) is shown for each data point, but

the ranges are so small that they only appear as black hash marks near the data point. 49

Figure 3.5 An example of boundary changes at block-group level between the 1990 and 2000 U.S. Censuses. Census 2000 (blue outlines with blue labels) and 1990 (transparent solid colors labeled with black fonts) boundaries were laid on top of a black-and-white aerial photos taken in Dundee Township in 2000. 52

Figure 4.1 Three case study sites (black box outlines) were sampled from Tomsk Oblast, Krasnoyarsk Krai and Irkutsk Oblast (black outline), centered at approximately 57.3°N/86.6°E, 57.3°N/96.1°E and 53.4°N/106.1°E. Source of eco-regions came from Olson *et al.* (2001). 60

Figure 4.2 User's and Producer's accuracy of the degraded land-cover change at the 240- (triangle), 480- (square) and 960-meter (solid circle) resolution for the Tomsk (a, b), Krasnoyarsk (c, d) and Irkutsk (e, f) sites. The reference is the 60-meter land-cover change dataset. Land-cover change codes are: 1 LOGGED, 2 BURNED, 3 INFESTED, 4 DEVELOPED, 5 REGEN I, 6 REGEN II, 7 SUCCESSION, 8 UNKNOWN, and 9 CONSTANT. 72

Figure 4.3 Proportion of individual land-cover changes identified at the degraded spatial resolutions in the Tomsk (a), Krasnoyarsk (b) and Irkutsk (c) sites. 74

Figure 4.4 Estimated Δbiomass (Mg C ha^{-1}) at 60-meter and degraded resolutions (a) and its RMSE with the 60-meter estimates at degraded resolutions (b). 76

Figure 4.5 Mean patch size (a), edge density (b), and mean shape index (c) of three case study sites. 77

Abstract

Changes in vegetation gross primary production (GPP) and forest aboveground standing biomass C (biomass) were investigated to better understand the impacts of human and natural disturbances on carbon uptake and storage in two northern hemisphere terrestrial ecosystems, which represent primarily forest-dominated and primarily urbanizing landscapes, respectively. Research focused on evaluating changes in (a) GPP in Southeastern Michigan, where the dynamics of vegetation carbon flux are tied closely to urbanization and human development characteristics; and (b) biomass in Eastern Siberia, where biomass changes are strongly affected by disturbance and regrowth.

Both projects exploited remotely sensed data and biophysical or ecosystem models to estimate GPP and biomass. Altering the scale of spatial data and summary units may generate different results. The scaling effects need to be characterized to evaluate scale-related uncertainties associated with carbon estimates. In Michigan, sensitivity of inferences about productivity trends among several development types to levels of aggregation in the Census housing data were examined from the block-group to county scales. In Siberia, impacts of changes in the remote sensing observational scale (i.e., sensor resolution) on the estimated biomass trends were analyzed at resolutions from 60 to 960 meters.

Results showed that GPP increased by 53 g C m^{-1} in Southeastern Michigan and biomass increased by 3.9 Mg C ha^{-1} in Eastern Siberia between 1990 and 2000, and that more productive landscapes resulted from tree-cover expansion and forest recovery,

respectively. These results corroborate previous findings of increased vegetation activity throughout the northern hemisphere in 1990s. With respect to scaling effects on carbon estimates, in Michigan, relationships between the estimated GPP trends and development types remained consistent across Census scales; and, in Siberia, degradation of remote sensing resolution resulted in the overestimation of changes in biomass by 9-69% at the 960-meter resolution. Results suggested that, for carbon analysis across broader geographic extents (e.g., regional- to national-scale estimation), coarser Census scales up to the county level may be used to evaluate carbon trends by development intensities, while remote sensing data at coarser resolutions may not maintain accuracy of the estimated carbon trends relative to finer resolution data.

Chapter I

Introduction

The carbon cycling of terrestrial ecosystems is affected significantly by human and natural disturbances (Vitousek 1994, Thornton *et al.* 2002, Krankina *et al.* 2005). In ecology, it is well known that CO_2 fluxes and plant carbon accumulation may change dramatically after stand-initiating disturbances, e.g., stand-replacing fire and forest clear-cut. Following these disturbances, productivity and biomass may increase from zero to an equilibrium state (Figure 1.1). However, because of the repeated human and natural disturbances (which at times are less severe, e.g., crown fire, insect infestation, and farming), such equilibrium state may not be reached. In addition, human land-use conversions such as building construction on the cleared forest land may completely prevent recovery of biomass. On the contrary, human activities such as agricultural abandonment may result in the regrowth of perennial woody species and, therefore, increase vegetation biomass. The roles of these human and natural disturbances in affecting ecosystem carbon dynamics are not yet fully understood, especially across different geographic and ecological settings.

To provide scientific evidence on impacts of human and natural disturbances, I investigated changes in vegetation primary production and biomass (C) in two representative landscapes in the northern hemisphere. One is located in Southeastern Michigan, U.S.A., and the other in Eastern Siberia, Russia. The two study areas are both

human-modified, but have different ecosystem types and land-use histories (Table 1.1). These distinctive landscapes formed a basis for comparing carbon changes in two mid-latitude northern hemisphere ecosystems. My research focused on impacts of urban and exurban development on gross primary production (GPP) in the Michigan study area, and effects of fire, insect and logging disturbances on aboveground standing biomass in the Siberian study area.

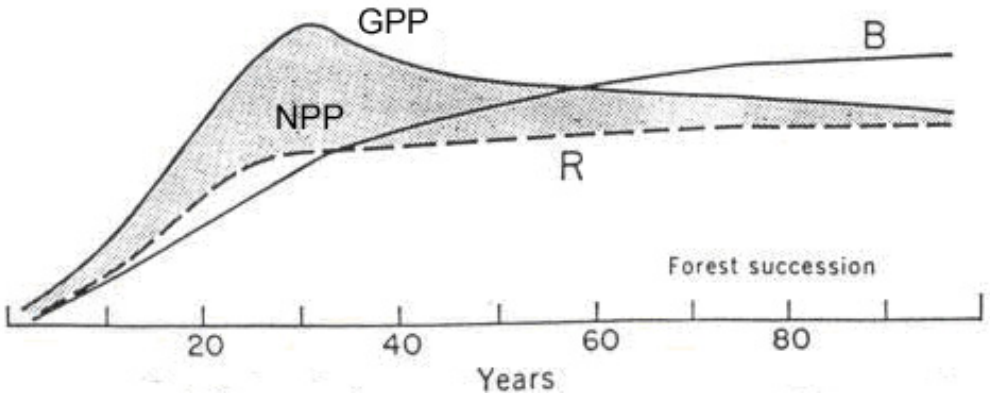

Figure 1.1 Changes in forest ecosystem gross primary production (GPP), net primary production (NPP), respiration (R) and biomass (B) after stand-initiating disturbances (adapted from Odum, 1969, Figure 1).

Table 1.1 Comparison of the two study areas.

Study area	Southeastern Michigan	Eastern Siberia
Climate	Temperate	Continental subarctic
Ecosystem type	Temperate hardwood forest	Taiga
Dominant land cover	Agriculture Urban settlement	Boreal forest
Dominant disturbance	Urbanization	Fire Insect infestation Logging

Remote sensing and Census data collected at multiple spatial and temporal resolutions were used to understand disturbance effects on GPP and biomass in the two

study areas. An important question that arises when using such data to understand carbon dynamics is associated with uncertainties of the carbon estimates due to spatial scaling of remote sensing and GIS data (Tate *et al.* 2000, Turner *et al.* 2004). I investigated two types of spatial scaling processes that are relevant to understanding the effects of disturbances on productivity and biomass in these landscapes: 1) changes in inference scale, referring to modification of statistical summary units such as Census block groups vs. tracts; and 2) changes in observation scale, referring to modification of observational units such as land-cover information extracted from 30-meter vs. 1-km satellite images. The type one scaling was examined for the Michigan study case (Chapter III), and type two for the Siberian study case (Chapter IV).

An overview of previous research on ecosystem carbon dynamics and scale dependences therein is discussed briefly in the remainder of this chapter. Chapter II concentrates on estimating changes in GPP (ΔGPP) in the urbanizing environment of Southeastern Michigan based on remotely sensed reflectance data and empirical plant light-use-efficiency parameters. Chapter III deals with the effects of the spatial scale of Census mapping units on inferences about relationships between the estimated ΔGPP and development types based on Census housing density. Chapter IV focuses on estimating changes in biomass (Δbiomass) resulting from disturbances and regrowth and the effects of remote sensing resolution on the estimates in Eastern Siberia. Chapter V summarizes research findings of the two study cases and discusses future directions extending from the presented research.

1.1 Productivity and biomass

Two types of primary production are used to describe the rate at which ecosystems produce organic matter through photosynthesis (Barnes *et al.* 1998). Gross primary production (GPP) is the total amount of carbon fixed by plants during the process of photosynthesis. Net primary production (NPP) is GPP less plant respiration. GPP indicates carbon uptake by plants from the atmosphere, and NPP describes the net flux of carbon between plants and the atmosphere. The net carbon gained through NPP is used to increase plant biomass or to supply herbivores and decomposers. Plant biomass is defined as the sum of dry mass of all plant tissues contained in a defined area and can be reported in its carbon equivalent (i.e., kg C ha^{-1}; Barnes *et al.* 1998). It can be partitioned into two parts, aboveground biomass (leaf, stem and pole) and belowground biomass (roots).

Both measures of primary production may be estimated using remote sensing observations (Gower *et al.* 1999, Running *et al.* 2000). At the global scale, GPP and NPP have been estimated based on biophysical parameters derived from vegetation indices (such as the normalized difference vegetation index, NDVI), global land-cover data, light-use-efficiency parameters, and carbon allometric equations (Running *et al.* 1999). Because previous studies showed that ratios of NPP/GPP are relatively constant for many plants (Waring *et al.* 1998) and because GPP is more directly related to remote sensing measurements, I analyzed GPP for the Michigan study case. This study contributes to the understanding of urbanization impacts on ecosystem carbon functions in a human-dominated environment.

Plant biomass can also be estimated with remote sensing techniques (Dong *et al.* 2003). Significant correlations were discovered between woody biomass calculated based

on forest inventory and satellite measurements of NDVI in several boreal and temperate forests across the mid- to high-latitude of northern hemisphere. However, it was also documented that correlation between satellite-based vegetation indices and biomass may be low due to saturation of the "sensed" reflectance at high end and variance in plant respiration rates (Wang *et al.* 2005, Zhao *et al.* 2006). Therefore, in the Siberian study, biomass was estimated using forest succession models and Landsat-based land-cover data. Results are expected to provide assessment of forest disturbance and regrowth events and their impacts on carbon cycles representative of the largely forested geographic extent of Siberian Russia.

1.2 Uncertainty of scale

In geography and ecology, scale is known to be an important factor affecting results of spatial analysis and modeling (Goodchild and Quattrochi 1997, Dungan *et al.* 2002, Aplin 2006). For example, the accuracy of land-cover classification changes when size (by area) of training samples is altered (Chen and Stow 2002). Estimates of NPP were shown to vary with the spatial resolution of imagery upon which maps of forest-age categories were generated (Turner *et al.* 2000). Spatial patterns of social segregation were found to change, depending on aggregation levels of Census data (Wong 2004). Many landscape pattern indices were found to be scale-dependent, meaning inferences about landscape pattern characteristics vary across the assessment scales (Wu 2004).

The nature of scaling problems differs depending on whether spatial data are represented as continuous fields (e.g., satellite images) or discrete geographic entities (e.g., Census units). In the case of remote sensing imagery, scaling is often expressed in forms of resolution degradation. With discrete data, scaling manifests as the so-called

modifiable areal unit problem (MAUP), which refers to the changed characteristics of a fixed observation at different geographic aggregation levels (Openshaw 1984). MAUP occurs where 1) areal data are aggregated to larger geographic units, e.g., aggregating Census population data from the block-group to tract level; 2) the boundaries of areal unit change, e.g., modification of Census tract boundaries between the two decennial U.S. Census dates; and 3) both aggregation and changes in boundaries take place, such as mapping socioeconomic data collected by Census or administrative units to watersheds or vice versa. In Chapter III, effects of changes in size and boundary of Census summary units on inferences about the relationship between changes in housing density and GPP were investigated. This study contributes to the understanding of scaling effects of Census mapping levels on interpreting biophysical parameters based on remote sensing observations.

Scale or resolution problems in remote sensing have been well defined in research back to the 1980s. Strahler *et al.* (1986) identified two different types of spatial resolutions in terms of the size of target objects in a remote sensing scene: 1) high resolution, where ground objects are larger than the pixel size of a sensor; and 2) low resolution, where ground objects are smaller than the pixel size of a sensor. By these definitions, classification of pure land-cover types is only possible in the high-resolution imagery. Mixture, present in low-resolution imagery, may exist in three forms: 1) multiple land-cover types occupy the same pixel, 2) gradual transition between two or more land-cover types occurs in a pixel, and 3) the land-cover type in a pixel is a "mixed" type, e.g., mixed conifer-deciduous forest (Fisher 1997, Brown 1998). All mixture problems result in difficulties in land-cover classification and biases in biophysical

estimators. Research efforts have sought after seeking optimal resolution(s) for imagery analysis such as land-cover classification, but no single resolution was found to be optimal for a given scene due to the divergent spatial patterns of ground objects (Marceau *et al.* 1994). Under the circumstances, it is important to document uncertainties of analysis due to the scale or resolution problem. In Chapter IV, effects of the changing remote sensing resolution on the estimate of biomass trends were evaluated. This study provides an assessment of estimation uncertainties due to spatial resolutions commonly used by satellite platforms such as Landsat and MODIS/AVHRR.

References

Aplin, P., 2006, On scales and dynamics in observing the environment. *International Journal of Remote Sensing* 27 (11): 2123-2140.

Barnes, B.V., Zak, D.R., Denton, S.R. and Spurr, S.H., 1998, *Forest Ecology*. Wiley, New York.

Brown, D.G., 1998, Classification and boundary vagueness in mapping presettlement forest types. *International Journal of Geographical Information Science* 12 (2): 105-129.

Chen, D.M. and Stow, D., 2002, The effect of training strategies on supervised classification at different spatial resolutions. *Photogrammetric Engineering and Remote Sensing* 68 (11): 1155-1161.

Dong, J., Kaufmann, R.K., Myneni, R.B., Tucker, C.J. and others, 2003, Remote sensing estimates of boreal and temperate forest woody biomass: Carbon pools, sources, and sinks. *Remote Sensing of Environment* 84: 393-410.

Dungan J.L., Perry J.N., Dale, M.R.T., Legendre, P. and others, 2002, A balanced view of scale in spatial statistical analysis. *Ecography* 25 (2): 626-640.

Fisher, P., 1997, The pixel: a snare and a delusion. *International Journal of Remote Sensing* 18 (3): 679-685.

Goodchild, M.F. and Quattrochi, D.A., 1997, Introduction: Scale, multiscaling, remote sensing, and GIS. In D.A. Quattrochi and M.F. Goodchild (Ed.) *Scale in Remote Sensing and GIS*. Bocan Raton: Lewis Publishers, pp. 1-13.

Gower, S.T., Kucharik, C.J. and Norman, J.M., 1999, Direct and indirect estimation of leaf area index, fAPAR, and net primary production of terrestrial ecosystems. *Remote Sensing of Environment* 70: 29-51.

Krankina, O.N., Houghton, R.A., Harmon, M.E., Hogg, E.H. and others, 2005, Effects of climate, disturbance, and species on forest biomass across Russia. *Canadian Journal of Forest Research* 35 (9): 2281-2293.

Marceau, D.J., Howarth, P.J. and Gratton, D.J, 1994, Remote sensing and the measurement of geographical entities in a forested environment. 1. The scale and spatial aggregation problem. *Remote Sensing of Environment* 49: 93-104.

Odum, E.P., 1969, Strategy of ecosystem development, *Science* 164: 262-270.

Openshaw, S. 1984. The Modifiable Areal Unit Problem, Concept and Techniques in Modern Geography 38. Norwich: Geo Books.

Running, S.W., Baldocchi, D.D., Turner, D.P., Gower, S.T. and others, 1999, A global terrestrial monitoring network integrating tower fluxes, flask sampling, ecosystem modeling and EOS satellite data. *Remote Sensing of Environment* 70: 108-128.

Running, S.W., Thornton, P.E., Nemani, R., and Glassy, J.M., 2000, Global terrestrial gross and net primary productivity from the Earth Observing System. In *Methods in ecosystem science*, O.E. Sala, R.B. Jackson, H.A. Mooney and R.W. Howarth (Eds.) (New York: Springer-Verlag), pp. 44-57.

Strahler, A.H., Woodcock, C.E. and Smith, J.A., 1986, On the nature of models in remote sensing. *Remote Sensing of Environment* 20: 121-139.

Tate, K.R., Scott, N.A., Parshotam, A., Brown, L., Wilde, R.H., Giltrap, D.J. and others, 2000, A multip-scale analysis of a terrestrial carbon budget – Is New Zealand a

source or sink of carbon? *Agriculture Ecosystems and Environment* 82 (1-3): 229-246.

Thornton, P.E., Law, B.E., Gholz, H.L., Clark, K.L., Falge, E., Ellsworth, D.S. and others, 2002, Modeling and measuring the effects of disturbance history and climate on carbon and water budgets in evergreen needleleaf forests. *Agricultural and Forest Meteorology* 113 (1-4): 185-222.

Turner, D.P., Cohen, W.B. and Kennedy, R.E., 2000, Alternative spatial resolutions and estimation of carbon flux over a managed forest landscape in Western Oregon. *Landscape Ecology* 15, 441-452.

Turner, D.P., Ollinger, S., Smith, M.L., Krankina, O. and Gregory, M., 2004, Scaling net primary production to MODIS footprint in support of Earth Observing System product validation. *International Journal of Remote sensing* 25 (10): 1961-1979.

Vitousek, P.M., 1994, Beyond global warming – ecology and global change. *Ecology* 75 (7): 1861-1876.

Waring, R.H., Landsberg, J.J. and William M., 1998, Net primary production of forests: a constant fraction of gross primary production? *Tree Physiology* 18:129-134.

Wang, Q., Adiku, S., Tenhunen, J. and Granier, A., 2005, On the relationship of NDVI with leaf area index in a deciduous forest site. *Remote Sensing of Environment* 94 (2): 244-255.

Wong, D.W.S., 2004, Comparing traditional and spatial segregation measures: A spatial perspective. *Urban Geography* 25 (1): 66-82.

Wu, J., 2004, Effects of changing scale on landscape pattern analysis: scaling relations. *Landscape Ecology* 19 (2): 125-138.

Zhao, M., S. W. Running, and R. R. Nemani. 2006. Sensitivity of Moderate Resolution Imaging Spectroradiometer (MODIS) terrestrial primary production to the accuracy of meteorological reanalyses. *Journal of Geophysical Research*, 111: G01002, doi:10.1029/2004JG000004.

Chapter II

Increasing Productivity in Urbanizing Landscapes

Abstract

In order to understand the impact of urbanizing landscapes on regional gross primary production (GPP), we analyzed changes in land cover and annual GPP over an urban-rural gradient in ten Southeastern Michigan counties between 1991 and 1999. Landsat and AVHRR remote sensing data and biophysical parameters corresponding to three major land-cover types (i.e., built-up, tree, and crop/grass) were used to estimate the annual GPP synthesized during the growing season of 1991 and 1999. According to the numbers of households reported by the U.S. Census in 1990 and 2000, the area settled at urban (>1 housing unit $acre^{-1}$), suburban (0.1-1 housing units $acre^{-1}$), and exurban (0.025-0.1 housing units $acre^{-1}$) densities expanded, while the area settled at rural (<0.025 housing units $acre^{-1}$) densities reduced. GPP in this urbanizing area, however, was found to increase from 1991 to 1999. Increasing annual GPP was attributed mainly to a region-wide increase in tree cover in 1999. In addition, the estimated annual GPP and its changes between 1991 and 1999 were found to be spatially heterogeneous. The exurban category (including constantly exurban and exurban converted from rural) was associated with the highest annual GPP as well as an intensified increase in GPP. Our study indicates that low-density exurban development, characterized by large proportions of vegetation, can be more productive in the form of GPP than the agricultural land it

replaces. Therefore, low-density development of agricultural areas in U.S. Midwest, comprising significant fractions of highly productive tree and grass species, may not degrade, but enhance, the regional CO_2 uptake from the atmosphere.

2.1 Introduction

Data from the U.S. Census has illustrated that much of the Eastern U.S. is undergoing significant deconcentration of population, leading to increased prevalence of low- to medium-density settlement across broad areas that were previously rural (Theobald, 2001). Nationwide, the area of land settled at densities of 1 house per 1 to 40 acres (i.e., suburban and exurban) increased about 500 percent from 1950 to 2000 (Brown *et al.*, 2005). This rate of suburban and exurban sprawl was shown to be more rapid in areas outside, but in proximity to, metropolitan regions. Based on these documented demographic changes, we identified two important environmental questions: 1) how does the density of residential development influence land-cover change? and 2) what are the impacts on primary production? Because residential development is affecting such large areas, i.e., low-density development occupied 15 times the area of dense urban settlements (Brown *et al.*, 2005), the answers to these questions could have significant consequences for regional and global carbon accounting.

In order to answer the two questions listed above, we analyzed changes in land cover and gross primary production (GPP) in ten Southeastern Michigan counties where suburban and exurban sprawl intensified between 1991 and 1999. Our approaches included: 1) mapping land-cover distribution and estimating annual GPP in each year, using Landsat and AVHRR remote sensing data; 2) deriving the pixel-wise changes in land-cover proportions and annual GPP between 1991 and 1999; and 3) characterizing

land-cover proportions and annual GPP by development-density categories (i.e., urban, suburban, exurban, and rural) and their changes by development-direction classes (i.e., conversions between any two development-density categories). We also examined sensitivity of the estimated GPP and its changes to different land-cover datasets and estimates of biophysical parameters. Our hypothesis was that low-density exurban development may not reduce annual GPP over the region as a whole at the scale of Census block group, because GPP that is reduced by increasing impervious surface and declining agriculture may be compensated through increasing areas of planted, regrowing, or maturing woody vegetation.

2.2 Background

2.2.1 Characterizing development density

In our study, we used housing-unit density instead of population density as the indicator of development density, because population counts ignore the effects of changes in household sizes (i.e., given a fixed population total, a smaller average household size implies more residential dwelling units, leading to a larger settlement area). Housing-unit density at the scale of Census block group equals the number of housing units divided by the land area of the block group. Housing-unit density does not directly take into account commercial and industrial land uses.

Based on Census housing-unit density, four categories of development density were defined, following Theobald (2001) and including: urban (>1 housing unit $acre^{-1}$, or less than 1 acre per housing unit), suburban (0.1-1 housing units $acre^{-1}$, or 1-10 acres per housing unit), exurban (0.025-0.1 housing units $acre^{-1}$, or 10-40 acres per housing unit), and rural (<0.025 housing units $acre^{-1}$, or more than 40 acres per housing unit). New

development associated with increasing housing-unit density may result in conversion from a lower to a higher development-density category (i.e., rural to exurban, exurban to suburban, and suburban to urban, etc).

2.2.2 Evaluating primary production

Two measures of primary production are widely used to describe ecosystem exchange of carbon between plants and the atmosphere. Gross primary production (GPP) is the total amount of carbon that is fixed by plants during the process of photosynthesis, and net primary production (NPP) is GPP less autotrophic respiration (i.e., plant respiration).

We used GPP as the measurement in this study for two reasons. First, compared to NPP, GPP can be more directly calculated from remotely sensed vegetation indices, given the more direct link of photosynthesis to plant's reflectance of shortwave radiation (e.g., Sellers, 1987). Second, estimates of GPP may have less uncertainty than NPP at local to regional scales. Uncertainties of estimation may increase when remote sensing measurements are coupled with ecological models that are required to calculate NPP (Zhao *et al.*, 2006). These models, in addition to estimating additional biophysical parameters, normally involve use of climate and/or soil data at degraded spatial resolutions. The increased uncertainty may prevent detection of real changes in productivity at the local to regional scale, such as those we aim to detect in our study.

GPP is difficult to measure directly but can be estimated with reflectance data collected by remote sensing instruments, based on light-use efficiency theory (Running *et al.*, 2000; Turner *et al.*, 2003). Light-use efficiency (LUE or ε) is defined as the ratio of total carbon uptake by green vegetation through photosynthesis (i.e., GPP) to the

absorbed photosynthetically active radiation (APAR). It is the energy-to-carbon conversion efficiency and varies among different species and communities. APAR can be calculated if incident solar radiation and reflectance of the intercepted vegetation canopy are known, and used to estimate GPP provided reasonable estimates of LUE are available.

2.3 Data and Methods

2.3.1 Study area

Our study region covers the Detroit-Ann Arbor-Flint consolidated metropolitan statistical area (CMSA), a ten-county region consisting of urban, suburban, exurban, and rural settlement densities (Figure 2.1). Previous research has documented relatively rapid development in the suburban and exurban parts of this region, despite declines within the cities of Detroit and Flint from the late 1950s to the present (MaCarthy, 1997; Theobald, 2001; Brown *et al.*, 2005). The 1990 and 2000 U.S. Census of population showed that the city of Detroit lost 8% of its residents, while the population of the CMSA increased 17%.

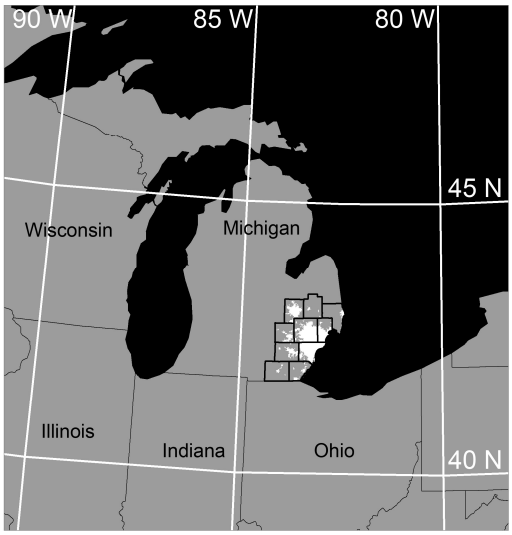

Figure 2.1 Study area covered ten Southeastern Michigan counties shown in thick black outlines, with the Detroit-Ann Arbor-Flint consolidated metropolitan statistical area displayed in white color.

According to household data of the Census, the total number of housing units declined 9% in city of Detroit, while it increased 21% in the CMSA. These opposing trends indicate continuing decentralization of the city, declining household sizes, and new development in suburban, exurban, and rural areas in 1990s.

2.3.2 Land-cover data

Landsat TM/ETM+ data collected during summers of 1991 and 1999 were geometrically registered and converted to six feature bands per dataset, which included Normalized Difference Vegetation Index (NDVI), Tasseled Cap brightness, Tasseled Cap wetness, ratio of band 4/band 7, texture of band 5, and texture of band 4/band 3. These six feature bands and a road-density map were used in unsupervised classification to generate 80 land-cover clusters in 1991 and 1999, respectively. We labeled and combined the clusters into five land-cover types, i.e., built-up, tree, crop/grass, water, and other (Table 2.1). Land-cover accuracy was assessed using randomly sampled 90-m × 90-m blocks of reference data that were scanned from aerial photographs at a resolution of 2 meters. The overall accuracies of the Landsat classification were 76.84% in 1991 and 82.27% in 1999. The users' accuracies were 71.48% (79.35%) for built-up, 70.59% (79.43%) for tree, and 81.71% (85.44%) for crop/grass in 1991 (1999). To calculate GPP at 1-km resolution, binary presence/absence maps were derived for built-up, tree, and crop/grass, respectively, in each year. Classes of water and other were not included in our calculations, as they were assumed to be relatively constant with respect to GPP. These 30-meter resolution binary land-cover data were then aggregated to create 1-km resolution grids to describe the percentage of built-up, tree, and crop/grass within each 1-km × 1-km cell, respectively.

Table 2.1 Definition of land-cover types.

Land-Cover Type	Description
Built-Up	Combines the high- and low-density residential/commercial lands. The former is composed of impervious surface in a large fraction (over 70% of cover) and scattered vegetation. The latter is a mixture of impervious surface in a smaller fraction (30-70% of cover) and increasing proportion of vegetation.
Tree	Combines broadleaf deciduous trees, needleleaf coniferous trees, and woody shrubs. Dominant tree species include oak, hickory, maple, beech, elm, ash, and cottonwood. According to the 1993 and 2001 Forest Inventory and Analysis (FIA) data, coniferous species occupied only 2-2.5% of the total forested area in the Southeastern Michigan region.
Crop/Grass	Combines agricultural farmlands and grassy fields. Dominant crops (by area) are corn, soybean, and hay (alfalfa). Over 90% of the cropland is rain-fed, according to the 2002 USDA Census of Agriculture.
Water	Combines rivers, lakes, and ponds.
Other	Combines wetlands, parks, and golf courses.

To evaluate the sensitivity of our analysis to alternative maps of land cover, we compared the results calculated using the land-cover data described above with estimates calculated using two other independent land-cover datasets that were also compiled from Landsat imagery. The datasets from 1992 National Land Cover Data (NLCD; Vogelmann *et al.*, 2001) and 1999-2000 Michigan Integrated Forest Monitoring Assessment and Prescription (IFMAP; Michigan Department of Natural Resources, 2003) replaced our 1991 and 1999 land-cover classification, respectively. Land-cover classes of the two datasets were grouped to match our definition of built-up, tree, and crop/grass before performing the comparative calculations of annual GPP.

2.3.3 Development density

We mapped development-density categories in 1990 and 2000 using housing-unit counts from the 1990 and 2000 U.S. Census of households. Census block-group

boundaries for both Census dates came from the Michigan Geographic Framework (MGF, 2005), which was created based on the 1994 Census Topologically Integrated Geographic Encoding and Referencing (TIGER) line files and improved with the U.S. Geological Survey (USGS) 1:12,000 Digital Ortho Quarter Quad (DOQQ) aerial photography. To derive the total land area that may be used in development, we removed water from the total area of each block group by using masks extracted from our 1991 and 1999 Landsat land-cover classification. We then calculated housing-unit density as the ratio of housing units to land area for each Census block group. Based on housing-unit density, Census block groups were classified into four development-density categories consisting of urban, suburban, exurban, and rural, as previously defined.

2.3.4 Annual GPP

We calculated GPP using methods based on light-use efficiency theory (Gower *et al.*, 1999). Daily GPP (GPP_d) equals the absorbed photosynthetically active radiation (APAR) multiplied by the energy-to-carbon conversion efficiency (i.e., LUE or ε), where APAR can be estimated from the incident radiation in photosynthetic wavelengths (PAR) multiplied by the fraction of PAR that is absorbed by plants (fPAR; Running *et al.*, 2004). We calculated GPP_d of each land-cover type ($GPP_{d,lc}$; g C m^{-2} day^{-1}) for each 1-km × 1-km cell by

$$GPP_{d,lc} = \%_{lc} \times \varepsilon_{lc} \times (PAR_d \times fPAR_{d,lc}) \quad (1)$$

where $\%_{lc}$ is the proportion of a given land cover (i.e., built-up, tree, or crop/grass) in each 1-km × 1-km cell, ε_{lc} is the LUE of the land-cover type (g C MJ^{-1}), PAR_d is the

daily incident PAR (MJ m^{-2} day^{-1}), and $fPAR_{d,lc}$ is the fraction of PAR_d absorbed by the land-cover type.

We used 1.8 and 2.2 g C MJ^{-1} for ε_{lc} of tree and crop/grass, respectively, based on the growing-season averaged LUE modeled by Turner and others (2003) for ecosystems comparable to our land-cover types, i.e., mixed conifer/deciduous forest (42.5°N, 72°W) and maize-dominated agricultural field (40°N, 88°W). For built-up, we estimated ε_{lc} to be 0.88 g C MJ^{-1} based on the estimated fractions of impervious surface (56%), trees (22%), and grass (22%) within our built-up areas. According to our land-cover classification, the high- and low-density residential/commercial types occupied approximately 30% and 70% of the built-up area, respectively. Given an estimated 70-100% and 30-70% of impervious surface for the high- and low-density residential/commercial types, respectively, the average fraction of vegetated cover was estimated at 44% for the built-up type. Assuming an even distribution of trees and grass on the vegetated surfaces and that $\varepsilon_{impervious}$ equals zero, ε_{lc} of built-up was set to 0.22 times the sum of ε_{tree} and $\varepsilon_{crop/grass}$, i.e., 0.88 g C MJ^{-1}. Certainly, the proportions of impervious surface, tree, and grass varied from place to place in real situation. Our assumption of the fixed proportions may introduce uncertainties in the estimated GPP, which, though not performed in the present study, can be evaluated by simulating different proportion combinations using statistical approaches such as Monte Carlo method.

The land-cover proportion ($\%_{lc}$) used in Equation (1) came from our binary land-cover data aggregated to 1-km resolution. PAR_d was calculated based on monthly mean

downward shortwave radiation (J sec^{-1} m^{-2}; NASA Data Assimilation Office, 1993) multiplied by the scalar 0.45 (i.e., the photosynthetically active proportion of the total incident shortwave electromagnetic radiation) and 24 hours in units of seconds. $fPAR_{d,lc}$ was calculated based on the biweekly 1-kilometer AVHRR NDVI (USGS EROS Data Center EDC, 1989), using an empirical MODIS NDVI-fPAR look-up table (LUT; Knyazikhin *et al.*, 1999). The AVHRR NDVI in the range 0.12 to 0.62 was first multiplied by 1.45 (Huete *et al.*, 2002) to convert it into units of MODIS NDVI, for the purpose of applying the MODIS-based LUT to estimate fPAR. We used NDVI-fPAR LUT values of broadleaf forest and broadleaf crop for our tree and crop/grass types, respectively. The LUT values for the built-up type was estimated with values for tree and crop/grass types, based on fractions of impervious surface (56%), trees (22%), and grass (22%) within our built-up type.

Once $GPP_{d,lc}$ was estimated for each land-cover type in each pixel according to Equation (1), the total daily GPP (GPP_d; g C m^{-2} day^{-1}) was derived by summing $GPP_{d,lc}$ values across land-cover types found within each pixel. Because this daily total was an estimate based on the maximum AVHRR NDVI over each 14-day time period, the accumulated daily GPP in each of the two-week time spans was derived by multiplying GPP_d by 14 days. We summed the accumulated biweekly GPP across the 11 two-week periods from early May to early October (during this period the average minimum daily temperature was 10°C and above), to estimate the pixel-wise growing-season GPP (GPP_{gs}; g C m^{-2} $year^{-1}$) as

$$GPP_{gs} = \sum_{tp=1}^{11}(14 \times \sum_{lc=1}^{3} GPP_{d,lc}) \qquad (2)$$

where lc is the three land-cover types and tp is the 11 two-week time periods corresponding to the biweekly AVHRR NDVI data over the growing season.

To evaluate the sensitivity of our estimation of GPP_{gs} to alternative LUE values, we calculated the growing-season GPP based on five additional combinations of ε_{lc} (Table 2.2). In total, we developed six representative estimates using 1) the average ε_{lc}, 2) the maximum ε_{lc}, 3) the minimum ε_{lc}, 4) ε_{lc} assuming the least productive tree and most productive crop/grass, and 5) ε_{lc} assuming the most productive tree and least productive crop/grass documented by Turner and others (2003); and 6) ε_{lc} used in Biome-BGC (BioGeochemical Cycles) that was applied to the global estimation of GPP and NPP with MODIS data (Running *et al.*, 2000).

Table 2.2 Light-use efficiency (LUE, g C MJ^{-1}) used in the estimation of daily GPP by land-cover types. LUE of built-up was approximated from values of tree and crop/grass, which came from Turner *et al.* (2003) for case 1-5 and Running *et al.* (2000) for case 6.

Case #	Built-Up	Tree	Crop/Grass
1	0.880	1.800	2.200
2	1.120	2.600	2.900
3	0.550	1.000	1.500
4	0.858	1.000	2.900
5	0.902	2.600	1.500
6	0.362	1.044	0.604

2.3.5 Changes in land cover and GPP by changes in development density

We compared maps of the 1990 and 2000 development-density categories to derive changes in development density, which we referred to as development-direction classes. Sixteen possible development directions consist of the constant classes (i.e., no conversions between development-density categories, including constantly urban,

constantly suburban, constantly exurban, and constantly rural), urbanizing classes (i.e., conversions from a lower to a higher development-density category, including urban converted from suburban, urban converted from exurban, urban converted from rural, suburban converted from exurban, suburban converted from rural, and exurban converted from rural), and ruralized classes (i.e., conversions from a higher to a lower development-density category, including rural converted from exurban, rural converted from suburban, rural converted from urban, exurban converted from suburban, exurban converted from urban, and suburban converted from urban).

If a class occupied less than 1% of the total study area, we combined it with other rare classes to create an "other conversion" class. The class of other conversion consisted of nine minor conversion directions and accounted for less than 3% of the total land area. The major development-direction classes included constantly urban (U), constantly suburban (S), constantly exurban (E), constantly rural (R), urban converted from suburban (UfromS), suburban converted from exurban (SfromE), and exurban converted from rural (EfromR). We calculated changes in land-cover proportions and GPP_{gs} for each Census block group, and then calculated the area-weighted average of these changes by eight development-direction classes (i.e., the seven major development-direction classes and the class of other conversion).

2.4 Results

Among the five land-cover types identified from the 30-meter Landsat imagery (Table 2.3), crop/grass dominated Southeastern Michigan by area, although it declined from 52% in 1991 to 49% in 1999. Tree was the second dominant land-cover type and increased from 20% in 1991 to 23% in 1999. Area of built-up occupied about 20% of the

total study area and showed little change between 1991 and 1999. Water and other land covers made up 8% of the total area with little change between 1991 and 1999.

Table 2.3 Area proportion (%) of the classified land-cover types in 1991 and 1999.

	Built-Up	Tree	Crop/Grass	Water	Other
1991	20.3	19.9	52.0	2.4	5.4
1999	20.2	22.8	48.7	2.8	5.4

Table 2.4 Land-cover proportions and annual GPP (GPP_{gs}) by development-density categories in 1991 and 1999. Values in parentheses are standard error of mean.

Development Density	Year	Land Area (acres)*	% Built-Up	% Tree	% Crop/Grass	GPP_{gs} (g C m^{-2} $year^{-1}$)
Urban	1991	508656	66.4	9.2	21.1	674
			(0.36)	(0.15)	(0.24)	(5.85)
	1999	588362	67.3	13.2	14.7	713
			(0.38)	(0.20)	(0.20)	(6.41)
Suburban	1991	905279	21.4	24.5	45.5	1613
			(0.55)	(0.42)	(0.65)	(15.18)
	1999	1039136	19.1	28.0	44.0	1715
			(0.60)	(0.48)	(0.65)	(16.58)
Exurban	1991	1351029	9.1	24.8	61.3	1992
			(0.38)	(0.80)	(1.05)	(17.88)
	1999	1359776	5.2	28.1	63.0	2128
			(0.36)	(0.79)	(0.98)	(12.91)
Rural	1991	540742	8.5	18.0	70.2	1930
			(1.08)	(0.88)	(1.35)	(33.54)
	1999	306350	7.2	15.6	72.1	2008
			(1.86)	(0.88)	(2.03)	(49.83)

* Area in 1991 and 1999 was calculated based on the Census housing-unit density in 1990 and 2000, respectively.

According to Census housing-unit density (Table 2.4), exurban was the dominant development-density category by area, followed by suburban and then urban (2000) or rural (1990). The total land area of the rural category decreased approximately 43% between 1990 and 2000, while the area of both urban and suburban categories increased

about 15-16%. The exurban category increased slightly (0.6% by area). In both years, crop/grass was the dominant land-cover type in suburban, exurban, and rural categories, while built-up dominated the urban category. Proportion of tree by area was higher in the suburban and exurban categories than in the urban or rural category. Proportion of built-up by area was the lowest in the exurban and rural categories. In terms of changes in land-cover proportions, tree increased from 1991 to 1999, except in the rural category. Built-up declined, except in the urban category. Crop/grass declined in the urban and suburban categories, and increased slightly in the exurban and rural categories.

In both 1991 and 1999, the estimated annual growing-season GPP (GPP_{gs}) was highest in exurban, followed by rural, suburban, and urban (Table 2.4). Over the entire study area, the pixel-wise GPP_{gs} increased 3% (or 53 g C m^{-2} $year^{-1}$) on average, from 1682 g C m^{-2} $year^{-1}$ in 1991 to 1735 g C m^{-2} $year^{-1}$ in 1999, which resulted in the total increment of GPP by 7×10^5 ton C. It increased as well in each of the development-density categories with different magnitude. The 1991-1999 increment was small for the urban category (39 g C m^{-2} $year^{-1}$), but large for the remaining categories (over 78 g C m^{-2} $year^{-1}$). Although estimates of GPP_{gs} varied with different assumptions for LUE values (Figure 2.2a), the annual GPP was consistently found to be 1) increasing between 1991 and 1999 and 2) highest in the exurban category and lowest in the urban category.

No major conversions from higher to lower development-density categories, i.e., ruralized classes, were found in our study area. Within the seven major development directions (Table 2.5), constant classes accounted for 79% of the total land area, while urbanizing classes with conversions from lower to higher development-density categories occupied 18% of the total land area. Within the constant classes, the constantly exurban

(E) and constantly suburban (S) classes dominated by area. Within the urbanizing classes, suburban converting from exurban (SfromE) and exurban converting from rural (EfromR) dominated by area.

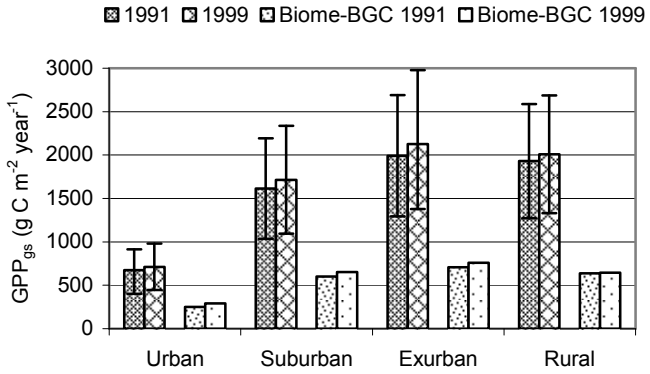

(a)

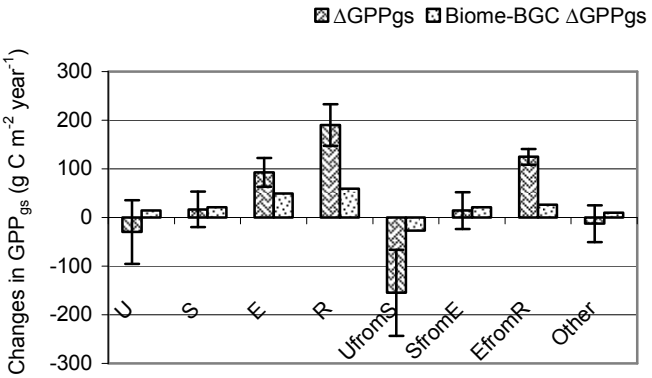

(b)

Figure 2.2 Annual GPP (GPP_{gs} , g C m^{-2} year $^{-1}$) by development-density categories (a) and its changes by development-direction classes (b). Error bars in (a) indicated the maximum and minimum annual GPP, which were calculated using the highest and lowest light-use efficiency (LUE) of tree and crop/grass adapted from Turner *et al.* (2003). Error bars in (b) indicated the maximum and minimum changes in annual GPP, which were calculated from the cross-combination of the highest and lowest LUE for tree and crop/grass adapted from Turner *et al.* (2003).

Increase in built-up proportion was high for suburban converted from exurban (SfromE) and urban converted from suburban (UfromS). Built-up proportion declined in the constantly rural (R), constantly exurban (E), and exurban converted from rural

(EfromR) classes. All of the development-direction classes experienced increased tree cover, with the greatest expansion of tree cover occurring in constantly exurban (E) and exurban converted from rural (EfromR). Crop/grass declined in all development-direction classes except constantly rural (R).

Table 2.5 Changes in land-cover proportions and annual GPP (GPP_{gs}) between 1991 and 1999 by development-direction classes.

Development Direction*		Percent of Land Area (%)	Changes in Land-Cover Proportions (%)			Changes in GPP_{gs} (g C m^{-2} $year^{-1}$)
			Built-Up	Tree	Crop/Grass	
Constant	U	14.0	4.7	2.7	-8.4	-29.91
	S	22.4	0.9	2.5	-4.0	16.67
	E	34.2	-2.8	4.4	-1.8	92.84
	R	8.4	-3.1	1.0	1.8	190.23
Urbanizing	UfromS	3.0	10.6	1.3	-12.9	-154.67
	SfromE	7.8	21.6	3.3	-3.4	14.28
	EfromR	7.3	-2.4	3.7	-1.2	124.68
Other Conversion		3.0	1.8	2.1	-5.1	-12.76

* U: constantly urban, S: constantly suburban, E: constantly exurban, R: constantly rural, UfromS: urban converted from suburban, SfromE: suburban converted from exurban, EfromR: exurban converted from rural, Other Conversion: the aggregation of nine minor conversion directions occupying less than 3% of the total land area.

The changes in annual GPP were positive except for the urban converted from suburban (UfromS) and constantly urban (U) classes. The constantly rural (R), exurban converted from rural (EfromR), and constantly exurban (E) classes were associated with the highest GPP increments from 1991 to 1999 (over 92 g C m^{-2} $year^{-1}$). The estimated magnitude of changes in annual GPP varied greatly depending on different sets of LUE values that were employed in analysis (Figure 2.2b). However, despite variations in magnitude, the general pattern of enhanced increment in the constantly rural (R), exurban converted from rural (EfromR), and constantly exurban (E) classes was relatively stable

for all assumptions of LUE values. Similarly, urban converted from suburban (UfromS) was always associated with the declining annual GPP.

2.5 Discussion

2.5.1 Increasing GPP in Southeastern Michigan

According to the Census housing-unit density in 1990 and 2000, Southeastern Michigan was characterized by increasing urbanization. Despite this trend towards more dense settlement patterns, our study found that the average regional GPP over the growing season increased rather than declined. Our investigation of changes in GPP by development-density categories (Table 2.4) and by development-direction classes (Table 2.5) showed that GPP increased in all categories and most classes, although more significantly in some than others. What has caused the increased GPP in this urbanizing environment? We examined the monthly average temperature and precipitation from the National Climatic Data Center Annual Climatological Summary during May through October in 1991 and 1999, and found no significantly different climate trends between the two years. Therefore, we suggest that the changes in GPP may be attributed to alterations in the incident solar radiation and land-cover proportions.

The temporal pattern of biweekly differences between 1991 and 1999 was very similar in the pixel-wise regional average of biweekly NDVI and estimated daily GPP (Figure 2.3). Given NDVI as an index of plant photosynthetic activity, Southeastern Michigan was greener in 1999 than in 1991 during the second half of the growing season. The increases in average NDVI during summer and autumn, 1999, may be attributed partially to the decline of incident solar radiation following the volcanic eruption of Mt. Pinatubo on June 15, 1991 (Ramachandran *et al.*, 2000). However, because no significant

decline of NDVI was found in 35-45°N North America between 1991 and 1992 (Tucker *et al.*, 2001), this increase in NDVI in the later growing season of 1999 may be attributed

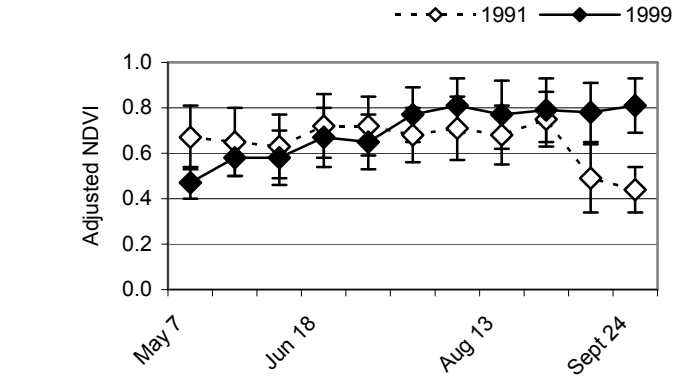

(a)

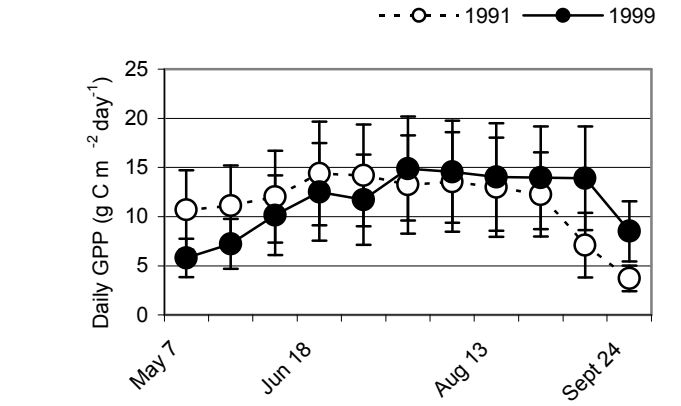

(b)

Figure 2.3 The pixel-wise regional average of (a) biweekly AVHRR NDVI (adjusted to units of MODIS NDVI) and (b) estimated daily GPP (GPP_d , g C m^{-2} day^{-1}) over the growing season between early May and early October. Dates on the x-axis corresponded to the starting date of each bi-weekly time period in 1991.

alternatively to an increasing fraction of deciduous tree species that develop full crowns in summer. We suggest that this is confirmed by our findings of increasing tree cover over the study area (Table 2.5).

The expansion of tree cover in urban and suburban areas most likely results from tree and shrub cover filling in open urban lots plus continuing growth of existing urban

trees. According to previous studies, the built infrastructure in the city of Detroit has been deteriorating since the 1960s due in part to the movement of the automobile and associated industries away from the city (McCarthy, 1997). Many old downtown neighborhoods, with the exception of scattered stable commercial and industrial areas, have been poorly maintained or abandoned with large areas of regrowing woody shrubs and trees (Ryznar and Wagner, 2001). Old suburbs might have experienced continuing growth and maturation of trees planted 30-60 years ago. The expansion of tree cover in the exurban areas was well documented in several concurrent land-cover/land-use change studies of the U.S. Upper Midwest (e.g., Bergen *et al.*, 2005). In Southeastern Michigan, where there are significant development pressures, this appears to come from a combination of agricultural abandonment and the expansion or maturation of tree cover in low-density residential areas (including where tree crowns block housing structures underneath).

Among the four development-density categories, exurban was associated with the highest annual GPP in both 1991 and 1999. This result agrees with previous findings of the highest estimated NPP in exurban area in the U.S. Midwest region (Imhoff *et al.*, 2004). Our study identified a mechanism for this fact in the form of a very high proportion of vegetated surface in exurban areas, i.e., 90-95% of the total land area in exurban was covered by tree and crop/grass. Although suburban contained the same proportion of tree cover, its built-up area was higher and crop/grass area was lower. Therefore, GPP in suburban areas was lower than exurban. GPP in urban areas was the lowest due to their large proportion of the built-up type. Depending on different values of LUE used in our analysis, rural was found either as productive as exurban or less

productive than both exurban and suburban categories. This contradiction results from the large proportion (over 70%) of crop/grass in rural areas. Given a major contribution from the crop/grass type, the estimated GPP in rural areas is very sensitive to LUE used for crop/grass.

Although annual GPP increased on average throughout the entire region, the different development directions behaved somewhat differently. Despite variation across the different LUE assumptions, the estimated change in annual GPP was generally large and positive for the constantly rural (R), exurban converted from rural (EfromR), and constantly exurban (E) classes, which were associated with increasing vegetation. The estimated change in annual GPP was high and negative or low and positive for the urban converted from suburban (UfromS), constantly urban (U), and suburban converted from exurban (SfromE) classes, which were characterized by growing built-up areas.

2.5.2 Uncertainties associated with land-cover data

The annual GPP was estimated based on land-cover, solar radiation, NDVI, and LUE. Any uncertainties associated with these datasets and parameters cause uncertainties in the estimates. For instance, the estimated GPP based on the highest LUE values from Turner and others (2003) can reach 3-4 times the estimation based on values from Running and others (2000). Despite differences in magnitude of estimates, the overall patterns were found to be stable for annual GPP by development-density categories and its changes by development-direction classes.

The estimation procedure also introduced uncertainties. For example, we used the daily GPP calculated from the maximum NDVI over each 14-day time period as the "daily" estimate of GPP for each day within the time period, whereas actual NDVI

changes day by day due to different plant phenology, reflectance of incident radiation, and cloud cover, etc. These variations were not taken into account given the AVHRR NDVI data prepared at a 14-day time step. However, to obtain the daily cloud-free NDVI data is nearly impossible and the 14-day composites are therefore commonly used data in remotely sensed productivity mapping and modeling. For calculation of daily GPP, we used the empirical MODIS NDVI-fPAR look-up table that was developed based on simulated data from the NOAA-11 AVHRR sensor. This might influence the magnitude of our estimated annual GPP in a systematic way throughout the entire study area. For estimation of biophysical parameters, we used constant estimates for the built-up type based on the average fractions of impervious surface, trees, and grass within it. Some variability in these fractions might be expected across the study area, which could be accounted for in future studies by using available estimates of impervious fraction (Yang *et al.*, 2003). Moreover, our estimated GPP did not include contributions from park or wetland land-cover types. Ecosystem dynamics might have changed within these two types. However, since parks are maintained by people and succession of wetland is a slow progress, we assumed that changes in these two land-cover types may be small during the time span of a decade.

Estimation uncertainties can also come from land-cover data in terms of classification errors (Figure 2.4). Although the estimated annual GPP continued to be the highest in the exurban development-density category, results of comparison showed that GPP was lower when NLCD (1992) and IFMAP (2000) were used to replace our 1991 and 1999 classifications, respectively, except for the rural type in 1991 and urban type in 1999. We found that higher estimates of GPP for rural areas in 1992 and for urban areas

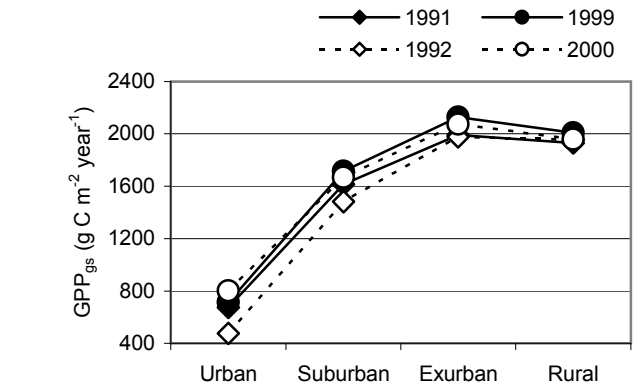

(a)

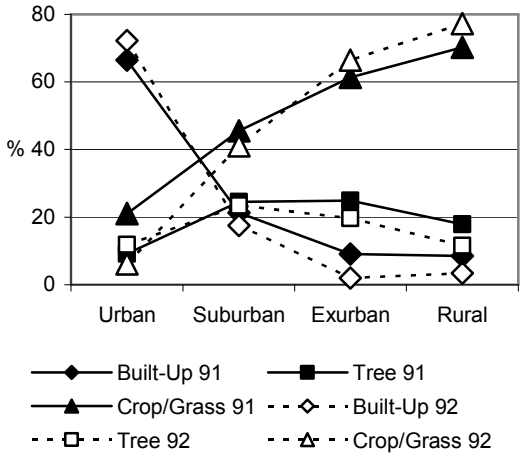

(b)

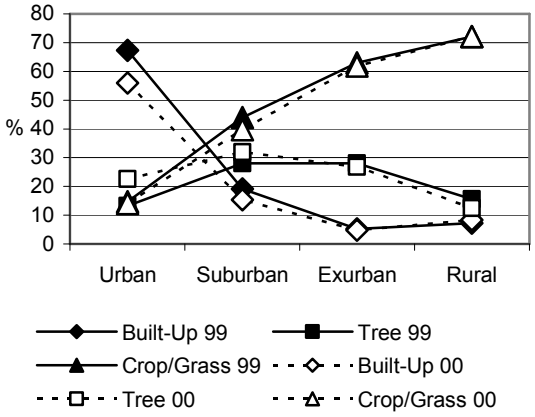

(c)

Figure 3.4 Comparison of results using our land-cover classifications (1991 and 1999) with those using the NLCD (1992) and IFMAP (2000) classifications: (a) estimated annual GPP (GPP_{gs}), (b) land-cover proportions in 1991 and 1992, and (c) land-cover proportions in 1999 and 2000.

in 2000 may have resulted from lower estimates of built-up by the alternative land-cover datasets. The differences in proportions of built-up between our dataset and that generated from the NLCD dataset (by combining low-density residential, high-density residential, and commercial, industrial or transportation) indicate a more relaxed definition of our built-up type, inclusive of more vegetation. Thus, proportion of built-up by our definition was higher in the suburban, exurban, and rural categories than the proportions derived by the NLCD definition.

2.5.3 Land-cover and GPP related to housing-unit density

In our study, development-density categories based on Census housing-unit density proved to be efficient in capturing land-cover/land-use characteristics along the urban-rural gradient (Figure 2.4b and 2.4c). When the maps derived from housing-unit density are associated with the land-cover classifications, urban densities are characterized by majority of built-up, with at least 30% impervious surface. Suburban and exurban densities are composed of less than 20% built-up and about 20-30% tree cover, where proportion of built-up is substantially lower in exurban than in suburban. Rural densities are characterized by majority of agricultural cropland or grassy fields. The estimated GPP and its changes also strongly relate to the four development-density categories and seven development-direction classes (Figure 2.2). Given the limited correlation between population density and vegetation fraction (Pozzi and Small, 2005), especially in the less densely-populated medium-to-small cities or densely-populated rural areas, the classification of urbanization based on housing-unit density instead of population density enables a stratification tied more closely to human land-use practices. This better facilitates the recognition of heterogeneous changes in landscape

characteristics and ecosystem functions due to human impacts at different levels of intensity.

2.6 Conclusions

We analyzed changes in land cover and gross primary production (GPP) between 1991 and 1999 using remotely sensed data and biophysical parameters for the Detroit-Ann Arbor-Flint consolidated metropolitan statistical area (CMSA) and vicinity, an urbanizing region of Southeastern Michigan. The pixel-wise changes were aggregated at the scale of the Census block group and then pooled by conversions between development-density categories that are defined from Census housing-unit density.

Despite the continuing urbanization characterized by conversions from lower to higher development densities, we found that the regional annual GPP increased in Southeastern Michigan. Increasing GPP was attributed mainly to the increased fraction of tree cover throughout the entire region, including the land maintained as urban and suburban between 1990 and 2000. Additionally, the increase in GPP was strengthened in exurban densities (including those converted from rural land), but was very weak or declining in suburban (including those converted from exurban land) and urban (including those converted from suburban land) densities. We conclude that 1) low-density exurban development increases GPP through the extended vegetation cover; and 2) further intensification of development reduces GPP by subsequent conversion of low-density exurban settlement to high-density urban or suburban settlement.

Human settlement can greatly modify the landscape composition and patterns. Understanding development impacts on carbon dynamics contributes not only to the global estimation of ecosystem production but also to the reliable prediction of future

climate. Our measurements of annual GPP and its changes in relation to different levels of urbanization over time provide a basis for the understanding of relationships between productivity and settlement development. Accurate scenarios of carbon budgets may be developed by incorporating localized ecosystem process models into this analysis to evaluate development impacts on NPP and biomass.

References

Bergen, K.M., D.G. Brown, J.F. Rutherford, and E.J. Gustafson. 2005. Change detection with heterogeneous data using ecoregional stratification, statistical summaries and a land allocation algorithm. *Remote Sensing of Environment* 97: 434-446.

Brown, D.G., K.M. Johnson, T.R. Loveland, and D.M. Theobald. 2005. Rural land use change in the conterminous U.S., 1950-2000. *Ecological Applications* 15 (6): 1851-1863.

Gower, S.T., C.J. Kucharik and J.M. Norman. 1999. Direct and indirect estimation of leaf area index, f(APAR), and net primary production of terrestrial ecosystems. *Remote Sensing of Environment* 70 (1): 29-51.

Huete, A., K. Didan, T. Miura, E.P. Rodriguez, X. Gao, and L.G. Ferreira. 2002. Overview of the radiometric and biophysical performance of the MODIS vegetation indices. *Remote Sensing of Environment* 83: 195-213.

Imhoff, M.L., L. Bounoua, R. DeFries, W.T. Lawrence, D. Stutzer, C.J. Tucker, and T. Ricketts. 2004. The consequences of urban land transformation on net primary productivity in the United States. *Remote Sensing of Environment* 89: 434-443.

Knyazikhin, Y., J. Glassy, J.L. Privette, Y. Tian, A. Lotsch, Y. Zhang, Y. Wang, J.T. Morisette, P.Votava, R.B. Myneni, R.R. Nemani, and S.W. Running. 1999. MODIS leaf area index (LAI) and fraction of photosynthetically active radiation absorbed by vegetation (FPAR) product (MOD15) algorithm theoretical basis document, URL: http://krsc.kari.re.kr/kari/sub/satellite/download/satellite_04/MODIS/atbd_mod15.pdf (last date accessed: 15 February 2006).

McCarthy, J. 1997. Revitalization of the core city: The case of Detroit. *Cities* 14 (1): 1-11.

Michigan Department of Natural Resources, Forest, Mineral and Fire Management Division. 2003. IFMAP/GAP Lower Peninsula Land Cover, URL: http://www.mcgi.state.mi.us/mgdl/?rel=thext&action=thmname&cid=5&cat=Land+Cover+2001 (last date accessed: 25 February 2006).

Michigan Geographic Framework. 2005. The Michigan Geographic Framework Program and Product Prospectus, URL: http://www.mcgi.state.mi.us/clearinghouse/Docs/MGF_History.pdf (last date accessed: 13 February 2006).

NASA Data Assimilation Office. 1993. Monthly Means of GEOS-1 Multiyear Assimilation, URL: http://disc.gsfc.nasa.gov/interdisc/readmes/assim54A_mo.shtml#202 (last date accessed: 25 February 2006).

Pozzi, F. and Small C. 2005. Analysis of urban land cover and population density in the United States. *Photogrammetric Engineering & Remote Sensing* 71 (6): 719-726.

Ramachandran, S., V. Ramaswamy, G. L. Stenchikov, and A. Robock. 2000. Radiative impact of the Mount Pinatubo volcanic eruption: Lower stratospheric response. *Journal of Geophysical Research* 105 (D19): 24,409-24,429.

Running, S.W., P. Thornton, E.R. Nemani, and J.M. Glassy. 2000. Global terrestrial gross and net primary productivity from the Earth Observing System, *Methods in*

Ecosystem Science (O.E. Sala, R.B. Jackson, H.A. Mooney, and R.W. Howarth, editors), Springer, New York, pp. 44-57

Running, S.W., R.R. Nemani, F.A. Heinsch, M. Zhao, M. Reeves, and H. Hashimoto. 2004. A Continuous Satellite-Derived Measure of Global Terrestrial Primary Production. *BioScience* 54: 547-560.

Ryznar, R.M. and T.W. Wagner. 2001. Using remotely sensed imagery to detect urban change: Viewing Detroit from space. *Journal of the American Planning Association* 67 (3): 327-336.

Sellers, P.J. 1987. Canopy reflectance, photosynthesis, and transpiration, II. The role of biophysics in the linearity of their interdependence. *Remote Sensing of Environment* 21 (2): 143-183.

Theobald, D.M. 2001. Land-use dynamics beyond the American urban fringe. *Geographical Review* 91: 544-564.

Tucker, C. J., D. A. Slayback, J. E. Pinzon, S. O. Los, R. B. Myneni, and M. G. Taylor. 2001. Higher northern latitude normalized difference vegetation index and growing season trends from 1982 to 1999. *International Journal of Biometeorology* 45: 184-190.

Turner, D. P., S. Urbanski, D. Bremer, S. C. Wofsy, T. Meyers, S. T. Gower, and M. Gregory. 2003. A cross-biome comparison of daily light use efficiency for gross primary production. *Global Change Biology* 9: 383-395.

U.S. Geological Survey, EROS Data Center. 1989. Conterminous U.S. biweekly NDVI composites. EROS Data Center. Sioux Falls, SD.

Vogelmann, J.E., S.M. Howard, L. Yang, C.R. Larson, B.K. Wylie, and N. Van Driel. 2001. Completion of the 1990s National Land Cover Data set for the conterminous United States from Landsat Thematic Mapper data and ancillary data sources. *Photogrammetric Engineering & Remote Sensing*, 67: 650-652.

Yang, L., C. Huang, C. G. Homer, B. K. Wylie, and M. J. Coan. 2003. An approach for mapping large-area impervious surfaces: synergistic use of Landsat-7 ETM+ and high spatial resolution imagery. *Canadian Journal of Remote Sensing*, 29 (2): 230–240.

Zhao, M., S. W. Running, and R. R. Nemani. 2006. Sensitivity of Moderate Resolution Imaging Spectroradiometer (MODIS) terrestrial primary production to the accuracy of meteorological reanalyses. *Journal of Geophysical Research*, 111: G01002, doi:10.1029/2004JG000004.

Chapter III

Census Scaling Effects on Inference of Productivity Trends

Abstract

We examined variance in the estimated changes in gross primary production (ΔGPP) as a function of spatial aggregation levels that corresponded to spatial units used by the U.S. Census. The estimate of ΔGPP in Southeastern Michigan was calculated based on satellite data and light-use-efficiency parameters. It was statistically summarized using a classification of Census units into eight development types at the block-group, tract, county-subdivision, and county levels. Results showed that inferences about the areal extents of development types were significantly dependent on Census scales, and that inferences about the relationships between ΔGPP and development types varied less with Census aggregation levels. This study implies that productivity trends may be estimated at coarse Census scales, though some of the development types may be missing at the coarsest levels.

Keywords: scale, modifiable areal unit problem, U.S. Census, gross primary production, Southeastern Michigan

3.1 Introduction

Scale, in this case meaning the level of details in data representations and analyses, has always been a necessary topic for research in ecology and geography. All monitoring and modeling of socioeconomic and environmental changes over time happen at some

scale. This chapter examines the effects of choice of spatial scale on inferences about the relationships between human settlement density and landscape productivity. Following Dungan et al. (2002), we distinguish two types of spatial scaling processes: alteration of observation scale (e.g., sampling plant species in plots sized 0.02 vs. 2 hectares) and alteration of inference scale (e.g., reporting biodiversity by townships vs. counties). The latter, i.e., spatial scaling of inference (SSI), is the main focus of this study.

SSI is conceptually analogous to the modifiable areal unit problem (MAUP), which refers to variance of statistical results due to changes in the size and zoning (i.e., shape) of geographic units (Openshaw 1984; Fotheringham and Wong 1991). MAUP studies initially addressed discrepancies in statistics and patterns at different spatial aggregation levels relevant to political or administrative units (Schneider et al. 1993; Wong 2004). However, it has also been considered in the field of remote sensing, where differences in the spatial resolution of sensors (or size of a pixel) are also regarded as a special case of MAUP (Jelinski and Wu 1996; Hay et al. 2001).

In this chapter, the term SSI refers specifically to changes in size and/or layout of geographic zones for summarizing an observation made at a fixed and finer spatial scale. For example, for observations of land-cover types identified on 30-meter resolution Landsat imagery, spatial scaling of inferences about land-cover percentage occurs when aggregation of land-cover information is made to the Census block-group vs. tract level, or when it is made using Census 1990 vs. 2000 tract boundaries. Perhaps more frequently occurring are the cases where both size and layout of the geographic unit change, such as mapping Census socioeconomic data by counties vs. watersheds (e.g., Goodchild, Anselin, and Deichmann 1993).

In this study, we evaluated the effects of SSI on interpretations of the relationships between changes in gross primary production (ΔGPP) and changes in housing density in the urbanizing environment of Southeastern Michigan between 1990 and 2000. According to the previous research (Chapter II), GPP increased region-wide over this period but at different rates by eight development types that were mapped at the Census block-group (BG) level (Zhao, Brown, and Bergen 2007). The present study concerns sensitivity of aggregated productivity estimates to the spatial scale of inference, i.e., alternative Census mapping units such as tracts (TR), county subdivisions (CS) and counties (CO). Because development types are the basis for summarizing ΔGPP statistically, their spatial patterns as a function of these alternative Census scales are also of interest in this study. Our null hypotheses included 1) the distribution of development types, which were mapped based on changes in Census 1990 and 2000 housing-unit densities, are independent of Census scales; and 2) the relationships between ΔGPP and development types vary with Census inference scales. This study will contribute to our understanding of the dependence of productivity estimates on modifiable aggregation units, and the appropriateness of Census aggregation level(s) for mapping trends in primary production at regional or larger geographic scales.

3.2 Study Area

Ten counties in Southeastern Michigan were selected for study, which include the Detroit-Ann Arbor-Flint metropolitan areas and less-densely populated exurban and rural areas (Figure 3.1). The average rate of growth in population and in housing units was approximately 12% and 17%, respectively, within the region between 1990 and 2000 (U.S. Census Bureau 2007). The most rapid growth was in Livingston County, which

experienced 36% increase in population and 41% increase in housing units. Wayne County, home to Detroit city, was the only county among the ten where population (-2%) and housing units (-0.8%) declined.

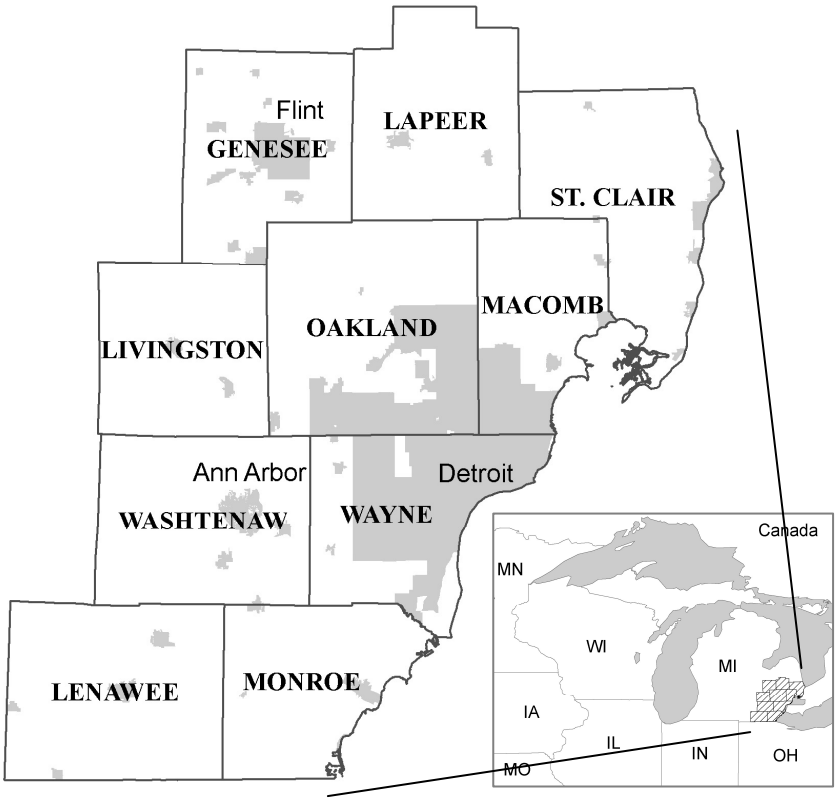

Figure 3.1 Study area included Detroit-Ann Arbor-Flint metropolitan (gray) and surrounding areas in ten Southeastern Michigan counties.

Corresponding to the regional growth of population and housing densities, changes in landscape composition and pattern have been detected based on remote sensing and natural resources inventory (Cifaldi et al. 2003; Bergen et al. 2005; Brown et al. 2007). According to the land-cover classification from the 1992 and 2001 National Land Cover Dataset (NLCD; Vogelmann et al. 2001, Homer et al. 2004), residential and commercial land uses increased from 15.7 to 20.5% of the total study area between early 1990s and early 2000s. However, the proportion of built-up area was found to be

relatively constant (approximately 20% of the study area) when analyzed using land-cover data developed specifically for this region between 1991 and 1999 (Zhao, Brown, and Bergen 2007). The expansion of built-up area resulted from urbanization and suburbanization processes was cancelled out through misclassification of built-up in areas where extension of tree crowns obscured buildings underneath. Tree-cover expansion was region-wide between 1991 and 1999, increasing from 1.0 to 4.4% of the area among different development types in 1991 (Zhao, Brown, and Bergen 2007). This was confirmed by trends of tree-cover percentage interpreted on 2-meter resolution aerial photos in 13 sampled townships in Southeastern Michigan (Brown et al. 2007). The increase in tree cover was due mainly to agricultural abandonment or conversion and tree-crown extension.

3.3 Data and Methods

The annual growing-season GPP was estimated based on synthesizing biweekly AVHRR NDVI, monthly solar radiation, and summertime Landsat land-cover data in 1991 and 1999 (Zhao, Brown, and Bergen 2007). GPP and its changes between the two years were mapped across Southeastern Michigan at 1-kilometer spatial resolution, determined by resolution of AVHRR NDVI data. In this study, ΔGPP is the observation at the finest scale, upon which inferences about its relationships to development types are drawn at different Census mapping unit levels.

Census data were acquired from two sources. Census boundary files came from Michigan Geographic Framework (MGF; Michigan Center of Geographic Information, 2007). These included boundaries of block groups, tracts, minor civil divisions (equivalent to Census county subdivisions) and counties. Boundaries of BG and TR

changed partially between the two U.S. Census dates, while geographic coverage of CS and CO units remained constant over the time period. Census housing data came from the U.S. Census Bureau (2007). Data of the total number of housing units for the ten counties were extracted from the Census Summary File 1 100-Percent Data (i.e., population and housing unit counts collected from all people and all housing units) at the BG, TR, CS and CO levels, respectively.

Four categories of development densities were adopted in this study (Theobald 2001): urban (<1 acre per housing unit), suburban (1-10 acres per housing unit), exurban (10-40 acres per housing unit) and rural (>40 acres per housing unit) densities. Two steps were involved to determine development density categories of each Census unit at each aggregation level. First, land area of a Census unit was calculated by subtracting water bodies classified in both 1991 and 1999 Landsat imagery from the total area of the Census unit. Second, development category was assigned to each Census unit based on area per housing unit (i.e., land area divided by number of housing units; hereafter "housing density", though strictly this quantity is the inverse of development density). The result was two maps of development densities at each inference scale, one for each Census date.

Changes in development densities during 1990-2000 were derived using two approaches. The first approach was to map categorical changes between the four development density classes based on calculation of a change matrix. Maps of the four discrete housing density categories were overlaid and, in total, 16 possible change directions were generated. They were grouped into eight development types consisting of four constant, three urbanizing and one "other" type (Table 3.1). The second approach for

analyzing changes in development densities was to map a continuous measure of change in housing density by Census units. At the CS and CO scales where boundaries of Census units remained constant between 1990 and 2000, differences in housing density between the two Census dates were derived by subtracting housing density values of the early date from values of the later date. At the BG and TR scales where Census boundaries changed, the differences in housing density between 1990 and 2000 were calculated in three steps: 1) we converted Census polygons from each year to a grid with a spatial resolution of 25 meters and assigned each grid cell a housing density value attached to the cell's corresponding Census polygon, 2) we calculated changes in housing density between the two years by subtracting the 1990 grid values from the 2000 grid values, and 3) we calculated the zonal average of changes in housing density by zones incorporating boundaries of both Census dates.

Table 3.1 Definition of development types

Type	Code	Definition
URBAN	U	Urban densities (<1 acre/housing unit) in both Census dates
SUBURBAN	S	Suburban densities (1-10 acre/housing unit) in both Census dates
EXURBAN	E	Exurban densities (10-40 acre/housing unit) in both Census dates
RURAL	R	Rural densities (>40 acre/housing unit) in both Census dates
URBANIZATION	UfromS	Suburban densities in 1990, changed into urban densities in 2000
SUBURBANIZATION	SfromE	Exurban densities in 1990, changed into suburban densities in 2000
EXURBANIZATION	EfromR	Rural densities in 1990, changed into exurban densities in 2000
OTHER	Other	Conversions other than the above categories

To evaluate scale dependence of changes in development densities, we performed accuracy assessment on the discrete development types and analyzed spatial autocorrelation of the continuous changes in housing density. Lower levels of accuracy and greater changes in spatial autocorrelation levels with the changing scale were both taken as indicators of scale dependence. An error matrix was calculated to assess accuracies of development types across Census scales. The map of eight development types at the Census BG level was used as reference, while those derived at the coarser Census levels were used as "classified" (Congalton and Green 1999). To measure spatial autocorrelation of changes in housing density, univariate global Moran's I was computed at each Census scale. The global Moran's I measures spatial autocorrelation based on the regression coefficient between values of spatial objects and those of their neighbors (Anselin 2003). It detects spatial patterns that can be classified as clustered (value near +1.0), random (value close to 0), or dispersed (value near -1.0) distribution. Significance of autocorrelation (as opposed to random pattern) is evaluated through comparing the actual Moran's I against the expected value resulting from hundreds of realization that randomly shuffles the value of spatial objects.

We assessed scale dependence of ΔGPP by calculating 1) the root mean squared error (RMSE) of ΔGPP at Census TR, CS, and CO levels, using estimates at the BG level as reference; and 2) the global Moran's I of ΔGPP at each Census scale. With respect to relationships between ΔGPP and development types across different Census scales, the average ΔGPP and its standard error of mean (s.e.m.) were calculated and reported by the eight development types. Estimates of ΔGPP across scales were compared among the eight development types on scatterplots.

3.4 Results

3.4.1 Changes in development densities

Patterns of development types varied among the levels of Census mapping units (Figure 3.2). Details of the geographic distribution of the eight development types disappeared gradually from the BG to CO scales. At the county level, only half of the

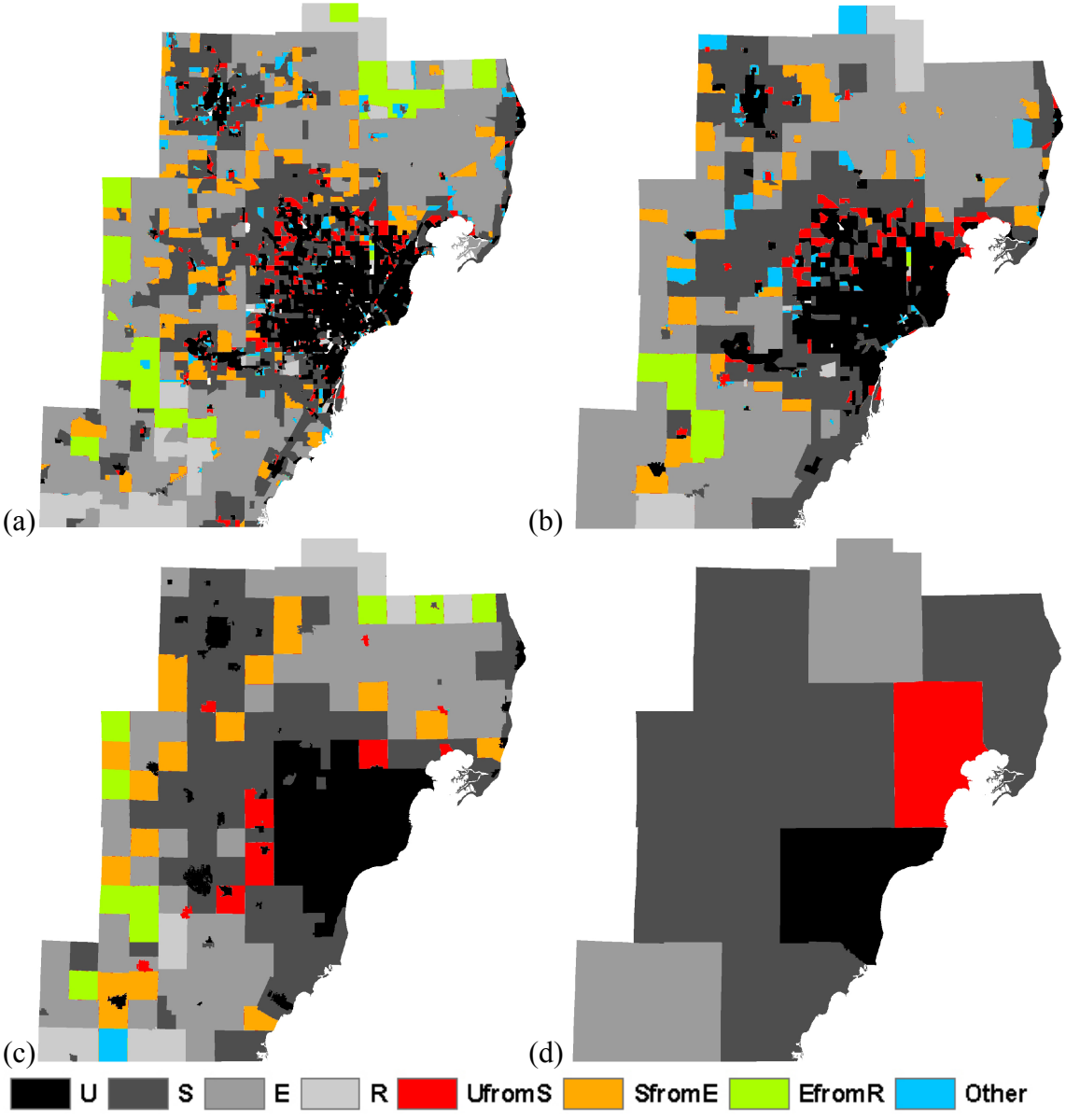

Figure 3.2 Development types and their distribution across the study area at the block-group (a), tract (b), county-subdivision (c), and county (d) levels.

eight development types remained, including URBAN, SUBURBAN, EXURBAN and URBANIZATION. Across the four scales, areal proportions of all development types at the CO level deviated most from values derived at the other Census scales (Figure 3.3). Proportions of SUBURBAN and EXURBAN by area varied most among the eight development types, and proportion of URBAN varied least.

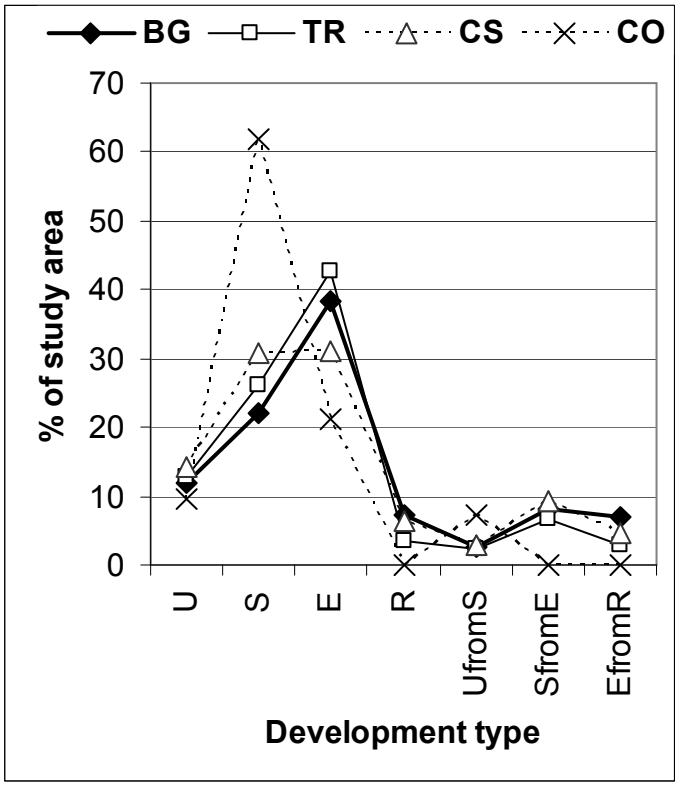

Figure 3.3 Proportion of the total study area by development types at four Census scales.

Accuracy assessment using the BG map as reference showed that the Kappa index of agreement (Pontius 2002) of development types at the coarser scales declined from 0.54 to 0.11 (Table 3.2). According to categorical producer's accuracies, URBAN was retained better than any other development types at the three coarser inference scales. Accuracies declined from TR to CO scales, expect for RURAL and EXURBANIZATION,

which increased at the CS level. Across the three scales, the constant types were generally better represented than the urbanizing types, with the exception of RURAL.

Table 3.2 Accuracy of categorization of development types (Kappa). Reference was the block-group level results.

Development Types	TR	CS	CO
U	0.88	0.80	0.33
S	0.69	0.57	0.28
E	0.62	0.44	0.09
R	0.28	0.70	0.00
UfromS	0.35	0.16	0.09
SfromE	0.20	0.12	0.00
EfromR	0.27	0.57	0.00
Other	0.14	0.00	0.00
Overall	0.54	0.49	0.11

As the scale was coarsened from BG to CO, the range of values of continuous change in housing density declined from 120 to 3 acres per housing unit. There was variability that indicated both decline and increase in housing density at the BG (-60 to +60 acre per housing unit) and TR (-45 to +20 acre per housing unit) levels. Changes were all negative at the CS (-10 to 0 acre per housing unit) and CO (-3 to 0 acre per housing unit) scales, indicating overall region-wide increases in development density. The spatial autocorrelation of changes in housing density was also shown to be scale-dependent, with significant spatial autocorrelation present at the BG scale and disappearing at coarser Census scales (Table 3.3).

3.4.2 Patterns of ΔGPP

Spatial autocorrelation of ΔGPP was significant at all four studied Census scales (Table 3.4). Values of Moran's I were all positive, implying clustered patterns of ΔGPP values. RMSE of the ΔGPP estimates was approximately 55.48, 63.55, and 56.96 g C m^{-2}

when aggregated from the 1-km cells to the TR, CS, and CO scales, respectively, using estimates at BG level as the reference.

Table 3.3 Spatial autocorrelation of changes in housing density across four Census scales. Changes in housing density were clustered at the block-group scale only.

Scale	Moran's I	Expected	Z score	Degree of cluster
BG	0.004362	-0.000088	4.052615	Cluster*
TR	0.000258	-0.000239	0.084211	Random
CS	0.000780	-0.003497	1.468345	Random
CO	-0.163006	-0.111111	-0.889657	Ramdom

* Sig. = 0.01

Table 3.4 Spatial autocorrelation of the estimated ΔGPP across four Census scales. Significant autocorrelation was found at all scales.

Scale	Moran's I	Expected	Z score	Degree of cluster
BG	0.025747	-0.000088	22.108073	Cluster*
TR	0.031839	-0.000239	4.892610	Cluster*
CS	0.095810	-0.003497	16.848802	Cluster*
CO	0.083068	-0.111111	3.234368	Cluster*

* Sig. = 0.01

Values of average ΔGPP for each of the eight development types were compared at each of the four inference scales (Figure 3.4). At the finest BG scale, RURAL, EXURBAN and EXURBANIZATION types were associated with the highest GPP increase between 1991 and 1999, with the increment estimated to be 198, 125, and 92 g C m^{-2}, respectively. Summarized at the BG scale, URBANIZATION was associated with the maximum decline of GPP, i.e., -154 g C m^{-2}. Although average values of ΔGPP for each development type differed from each other by Census scales (s.e.m. <1 g C m^{-2}), the overall pattern of relationships between ΔGPP and development types was retained across the four Census scales. The RURAL, EXURBAN and EXURBANIZATION types always corresponded to largest

increases in GPP, regardless of Census inference scales, while GPP of the URBANIZATION type declined the most at all scales. At the CO level it is worthwhile noting that three development types were missing (Figure 3.2); and that, for the remaining development types, the pattern of relationships between ΔGPP and development types remained the same. The CO-level ΔGPP values deviated further from statistics drawn at other Census scales. At the BG, TR and CS levels, relatively stable estimates of ΔGPP were found for the URBAN and SUBURBAN types.

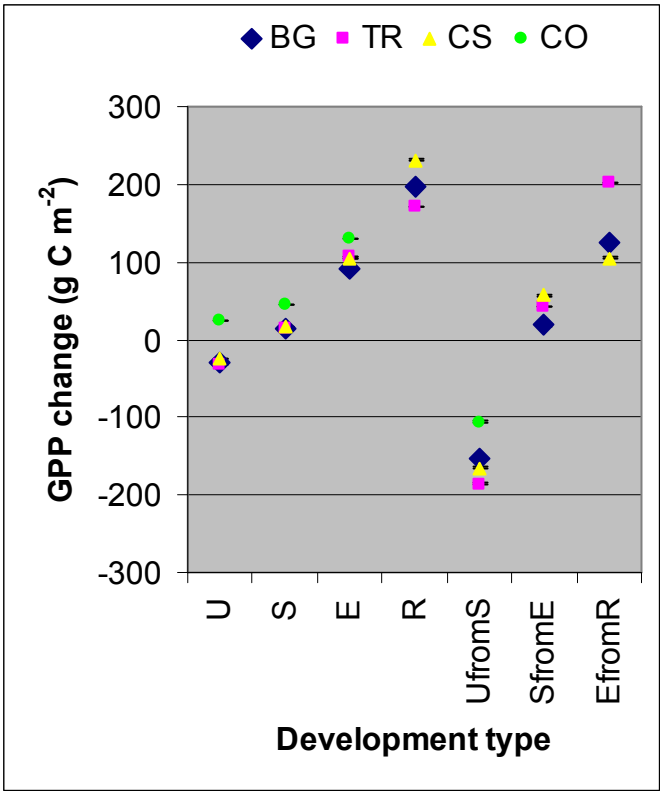

Figure 3.4 The estimated ΔGPP by development types at four Census inference scales. Relationships between ΔGPP and development types were retained similar across all Census levels. The standard error of mean (s.e.m.) is shown for each data point, but the ranges are so small that they only appear as black hash marks near the data point.

3.5 Discussion

3.5.1 Scale dependence of housing and GPP inference

In this study, inferences about changes in area covered by different development densities were shown to vary with Census aggregation scales. Changes in housing density were clustered spatially by Census block groups. This pattern of spatial autocorrelation was missing in larger Census units. This implies that SSI resulted in biased interpretation of spatial patterns of Census housing characteristics. The result corroborates previous research findings, where patterns of socioeconomic data changed with geographic aggregation units. For example, an analysis on patterns of cancer distribution for five selected U.S. states showed that, among four available aggregation levels ranging from state to Census minor civil division (MCD), spatial clusters of cancer were only identified at the finest scale, MCD (Schneider et al. 1993). A study on social segregation also showed that measurement indices were sensitive to changes in scale of inference, and that smaller areal units at the Census block-group level tended to capture higher segregation patterns than larger areal units at the Census tract level (Wong 2004).

Inferences about spatial patterns of ΔGPP and the relationship of ΔGPP to development types were not found to be scale dependent across the Census block-group to county levels. Compared to changes in development densities, spatial patterns of ΔGPP were less sensitive to Census scales. At all inference scales, significant spatial autocorrelation of ΔGPP was identified. This indicates that inferences about spatial patterns of ΔGPP were not dependent on Census unit sizes ranging from block groups to counties. Despite scale dependence of development types (Table 3.2), the rank of different development types in terms of ΔGPP remained relatively constant across all

Census scales, even at the county level where three development types disappeared (Figure 3.4). This result implies that inferences about relationships between productivity trends and changes in human development density remained consistent across Census scales finer than county level (including counties).

The inconsistency between changes in housing density and changes in GPP, with respective to scale dependence, may result from different base observational scales. The minimum mapping unit for housing density is Census units varying across inference scales, while it is the fixed 1-km resolution grid cell for GPP. The relatively stable relationship between ΔGPP and development types suggests correlation between the two variables, which implies similar scaling impacts of Census aggregation units on the two variables. Cloud-contaminated Census units were all included in the present analysis, so the average GPP for some Census units could be based on a very small number of pixels. Future work is need to exclude Census units with over 50% cloud coverage (as was done in the analysis in Chapter II) for the comparison of development and ΔGPP across scales.

We also found that it was not always true that estimates of ΔGPP at the TR level are more similar than estimates at the CS level to the block-group estimates (e.g., EXURBAN and URBANIZATION, Figure 3.4), though tracts held more detailed patterns of changes in development densities than county subdivisions (Figure 3.2). Compared to the CS level, values of the CO-level ΔGPP estimates by development types deviated more from the BG-level estimates (Figure 3.4); however, the region-wide average of RMSE of the ΔGPP estimates compared to the BG-level data was lower at the county scale (57 g C m^{-2}) than at the finer county-subdivision scale (64 g C m^{-2}). This indicates that scaling effects of Census inference scale are more complex than expected, in the sense that

coarser scale estimates are not necessarily more divergent than finer scale estimates when they are both compared to the block-group estimates.

3.5.2 Mismatching Census boundaries

Because this study of scaling effects evaluated changes in housing density and GPP over time, modification of Census boundaries at the block-group and tract levels meant complicated interpretations of the differences in estimates across the four scales (BG, TR, CS and CO). For example, as shown in a carefully selected portion of Dundee Township in Monroe County, the extents of Census block groups in 1990 differed greatly from those in 2000 (Figure 3.5). BG 1 and 2 covered more low-density exurban/rural settings in 2000 than 1990; therefore, development density was shown to decline in the green (from 1.54 to 0.39 housing units per acre) and olive green (from 1.01 to 0.74 housing units per acre) areas.

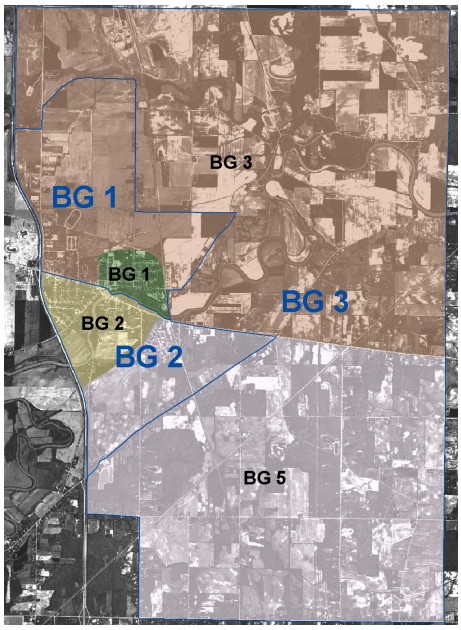

Figure 3.5 An example of boundary changes at block-group level between the 1990 and 2000 U.S. Censuses. Census 2000 (blue outlines with blue labels) and 1990 (transparent solid colors labeled with black fonts) boundaries were laid on top of a black-and-white aerial photos taken in Dundee Township in 2000.

The changes in boundaries of the housing density data may introduce errors into the map of development types (e.g., small polygons appeared to lose housing units per acre and would be classified as the "urban converted to suburban" type, because their extents changed between the two Census dates), which may propagate to estimates of ΔGPP for the corresponding Census block-group and tract units. As a result, a question arose whether productivity trends estimated at the block-group or tract scale are accurate and may be used as reference to assess estimates made at coarser Census scales. In this study we did not try to fix this problem given two considerations. To adjust Census housing data fitting to the changed Census boundaries, ancillary data such as demographic information finer than the block-group scale are required (Martin 2003). Alternatively, high-resolution remote sensing may help us to interpolate housing density in Census units with changed boundaries. However, although correlation was found between Census housing data and satellite-based residential classification in several urban areas (Chen 2002; Li and Weng 2005), strength of the correlation was also shown to be limited by housing densities and/or house types (Harvey 2002; Guindon, Zhang, and Dillabaugh 2004).

The mismatching Census boundaries existed only at the block-group and tract levels in the Southeastern Michigan study area between the 1990 and 2000 U.S. Censuses. They occurred more often in less-densely populated areas. This might provide an explanation for the fact that URBAN is the most stable one among all development types with respect to estimates of changes in both housing density and GPP across all Census inference scales (Figure 3.3 and 3.4).

3.6 Conclusions

Sensitivity of the estimated productivity trends to Census aggregation scales was investigated along an urban-rural gradient in Southeastern Michigan. Changes in primary production were statistically summarized by development types that were inferred at four Census levels from the finest block-group to coarsest county scales. Although the areal extents of development types were shown to vary across Census scales, estimates of ΔGPP and relationships between ΔGPP and development types were found to be less dependant on Census scales. Values of ΔGPP were closer to the block-group estimation at the tract or county-subdivision scales than at the county scale. Although several types of changes in housing density were not detectable at the county scale, the overall trends of ΔGPP by different development types were consistent with finer scale analyses. The results imply that all of the four studied Census scales can be used to interpret productivity trends between the decennial U.S. Censuses. In future research of productivity trends across the entire U.S., county and county subdivision may potentially be good candidate scales of inference.

References

Anselin, L. 2003. GeoDa^{TM} 0.9 User's Guide, https://www.geoda.uiuc.edu/documentation/manuals (last accessed 19 July 2007).

Bergen, K. M., D. G. Brown, J. F. Rutherford, and E. J. Gustafson. 2005. Change detection with heterogeneous data using ecoregional stratification, statiscal summaries and a land allocation algorithm. *Remote Sensing of Environment* 97: 434-446.

Brown, D. G., D. T. Robinson, L. An, J. I. Nassauer, M. Zellner, W. Rand, R. Riolo, S. E. Page, and B. Low. 2007. Exurbia from the bottom-up: Confronting empirical challenges to characterizing a complex system. *Geoforum* (forthcoming)

Chen, K. 2002. An approach to linking remotely sensed data and areal census data. *International Journal of Remote Sensing* 23 (1): 37-48

Cifaldi, R. L., D. Allan, J. D. Duh, and D. G. Brown. 2003. Spatial patterns in land cover of exurbanizing watersheds in southeastern Michigan. *Landscape and Urban Planning* 66: 107-123.

Congalton, R. G. and K. Green. 1999. *Assessing the Accuracy of Remotely Sensed Data: Principles and Practices*. Boca Raton, FL: Lewis Publishers.

Dungan J. L., J. N. Perry, M. R. T. Dale, P. Legendre, S. Citron-Pousty, M. J. Fortin, A. Jakomulska, M. Miriti, and M. S. Rosenberg. 2002. A balanced view of scale in spatial statistical analysis. *Ecography* 25 (2): 626-640.

Fotheringham, A.S. and D. W. S. Wong. 1991. The modifiable areal unit problem in statistical analysis. *Environment and Planning* A 23: 1025-1044.

Goodchild, M. F., L. Anselin, and Deichmann, U., 1993, A framework for the areal interpolation of socioeconomic data. *Environment and Planning* A, 25: 383-397.

Guindon, B., Y. Zhang, and C. Dillabaugh. 2004. Landsat urban mapping based on a combined spectral-spatial methodology. *Remote Sensing of Environment* 92: 218-232.

Harvey, J. T. 2002. Estimating census district populations from satellite imagery: some approaches and limitations. *International Journal of Remote Sensing* 23 (10): 2071-2095.

Hay, G. J., D. J. Marceau, P. Dubé, and A. Bouchard. 2001. A multiscale framework for landscape analysis: Object-specific analysis and upscaling. *Landscape Ecology* 16: 471-490.

Homer, C., C. Huang, L. Yang, B. Wylie, and M. Coan. 2004. Development of a 2001 National Landcover Database for the United States. *Photogrammetric Engineering and Remote Sensing*, Vol. 70 (7): 829-840.

Jelinski, D. and J. Wu. 1996. The modifiable areal unit problem and implications for landscape ecology. *Landscape Ecology* 11 (3): 129-140.

Li G. and Q. Weng. 2005. Using Landsat ETM+ imagery to measure population density in Indianapolis, Indiana, USA. *Photogrammetric Engineering and Remote Sensing* 71 (8): 947-958.

Martin, D. 2003. Extending the automated zoning procedure to reconcile incompatible zoning systems. *International Journal Geographical Information Science* 17 (2): 181-196

Michigan Center for Geographic Information. 2007. The Michigan Geographic Framework Program and Product Prospectus (MGF Version 6), http://www.michigan.gov/documents/CGI_frmwkdoc06_169807_7.pdf (last accessed 18 July 2007).

Openshaw, S. 1984. The Modifiable Areal Unit Problem, Concept and Techniques in Modern Geography 38. Norwich: Geo Books.

Pontius, R. G. 2002. Statistical methods to partition effects of quantity and location during comparison of categorical maps at multiple resolutoins. *Photogrammetric Engineering and Remote Sensing* 68 (10): 1041-1049.

Schneider, D., M. R.Greenberg, M. H. Donaldson, and D. Choi. 1993. Cancer clusters: The importance of monitoring multiple geographic scales. *Social Science and Medicine* 37 (6): 753-759.

Theobald, D. M. 2001. Land-use dynamics beyond the American urban fringe. *Geographical Review* 91: 544-564.

U.S. Census Bureau. 2007. Decennial Census, http://factfinder.census.gov/servlet/DatasetMainPageServlet?_lang=en (last accessed 23 May 2007)

Vogelmann, J. E., S. M. Howard, L. Yang, C. R. Larson, B. K. Wylie, and N. Van Driel. 2001. Completion of the 1990s National Land Cover Data set for the conterminous United States from Landsat Thematic Mapper data and ancillary data sources. *Photogrammetric Engineering and Remote Sensing*, 67: 650-652.

Wong, D. W. S. 2004. Comparing traditional and spatial segregation measures: A spatial perspective. *Urban Geography* 25 (1): 66-82

Zhao, T., D. G. Brown, and K. M. Bergen. 2007. Increasing gross primary production (GPP) in the urbanizing landscapes of Southeastern Michigan. *Photogrammetric Engineering and Remote Sensing* 73 (10) (forthcoming)

Chapter IV

Changes in Biomass at Landsat to AVHRR Resolutions

Abstract

We investigated the influence of remote sensing spatial resolution on estimates of forest biomass change due to disturbance and regrowth in three study sites (each corresponding to a Landsat scene) in Eastern Siberia. Changes in aboveground standing biomass (Δbiomass) were estimated using 1990 and 2000 Landsat 60-meter land-cover data and biomass densities simulated by the FAREAST model. Land-cover data were then progressively degraded to 240, 480 and 960 meters, and land-cover change (LCC) proportions and Δbiomass were derived at each of the coarser resolutions. Scale dependences of Δbiomass and LCC patch characteristics were analyzed. Estimated at 60-meter resolution, biomass increased in two sites (3.0-6.4 Mg C ha^{-1}) and declined slightly in one site (0.5 Mg C ha^{-1}). Between 31 and 64% of logging, small fires, and development disturbances were lost as the resolution was degraded, resulting in higher estimates of biomass increase. Fires at a third site were larger in size, and the over-represented burned area resulted in over-estimation of biomass decrease at coarser resolutions. Results indicate that Δbiomass values may be amplified in either direction as resolution is degraded, depending on the average patch size of disturbances and that the error of Δbiomass estimates also increases at coarser resolutions.

Keywords: scale, resolution, land-cover change, biomass, disturbance, forest succession, FAREAST model, Eastern Siberia

4.1 Introduction

By area, the Russian Federation is the world's largest country. Approximately one-half of its territory is covered by boreal and temperate forests, and these comprise approximately 20% of world forest lands (FAO, 2005). The largest part of this Russian forest is in Siberia. In addition to its leading role in world forest resources, Siberia is increasingly influential in global carbon accounting (Bergen *et al.* 2003, Mayer *et al.* 2005, Schiermeier 2005). To quantify carbon storage and flux in Siberian forest ecosystems, several research projects have been conducted and these have yielded inconsistent conclusions regarding Siberia's role as a sink or source of carbon dioxide (Schulze *et al.* 1999, Lloyd *et al.* 2002, Röser *et al.* 2002, Vedrova *et al.* 2002). One of the sources of uncertainty is related to the availability of datasets on forest disturbance and regrowth. Logistically, these data are very difficult to compile using conventional forest inventory methods over large and remote boreal regions.

Remote sensing techniques facilitate the measurement of dynamic forest changes across the vast geography of Siberia. During the last several decades, satellite imagery has been employed broadly to monitor and evaluate forest cover, standing biomass, and natural or human-induced disturbances in Siberian ecosystems (Bartalev *et al.* 2003, Kharuk *et al.* 2003, Wagner *et al.* 2003, Soja *et al.* 2004, Sukhinin *et al.* 2004, Krankina *et al.* 2005, George *et al.* 2006). The resulting products, used in conjunction with field investigations, carbon allocation equations and ecological models, can be an efficient basis for estimating carbon budgets at the regional to national scales. However, because

most affordable continuous satellite data are coarser than 250 meters, there is need to understand sample bias in estimates based on these satellite data. Sources for such bias may originate from loss of spatial details depending on the relative patch sizes of land cover and land-cover change.

Although research on scaling issues in remote sensing can be dated back to the 1980s (Strahler *et al.* 1986, Atkinson and Curran 1997, Asner *et al.* 2002, Aplin 2006), less work has been done until recently to examine uncertainties of satellite-based estimation of biomass or ecosystem productivity. In North America, researchers found that estimates of net primary production (NPP) and net ecosystem production (NEP) in a Pacific Northwest forest decreased when calculated at progressively degraded spatial resolutions from 25 meters to 1 kilometer (Turner *et al.* 2000). In contrast, a study in African savanna ecosystems showed that aggregation of heterogeneous landscapes resulted in increased estimates of NPP (Caylor and Shugart 2004).

In this study, we examined spatial scaling effects on the estimated changes in biomass (Δbiomass) due to disturbance and regrowth at three sample sites in Eastern Siberia. The objectives of the study were to 1) quantify Δbiomass resulting from disturbances, forest regeneration and forest succession between image dates of 1990 and 2000; 2) evaluate uncertainties of these satellite-based estimates at degraded spatial resolutions equivalent to the pixel size of MODIS (Moderate Resolution Imaging Spectroradiometer) and AVHRR (Advanced Very High Resolution Radiometer) sensors; and 3) explore the relationships between uncertainties of the estimated Δbiomass and patch characteristics of land-cover dynamics. The results of the last objective should provide insight into the spatial characteristics of disturbance and regrowth, and the

uncertainties associated with Δbiomass estimates at the spatial resolutions of different remote sensors for Siberian forests.

4.2 Study Area and Data

4.2.1 Study area

The study area included three case study sites, each the size of a Landsat scene footprint, sampled from Tomsk Oblast, Krasnoyarsk Krai and Irkutsk Oblast in Eastern Siberia (Figure 4.1). In this region, the climate is continental with long, severe winters and short, warm summers, and over 40% of the annual precipitation occurs in summer from June to August (WMO 2007). The Tomsk, Krasnoyarsk and Irkutsk sites occur on a

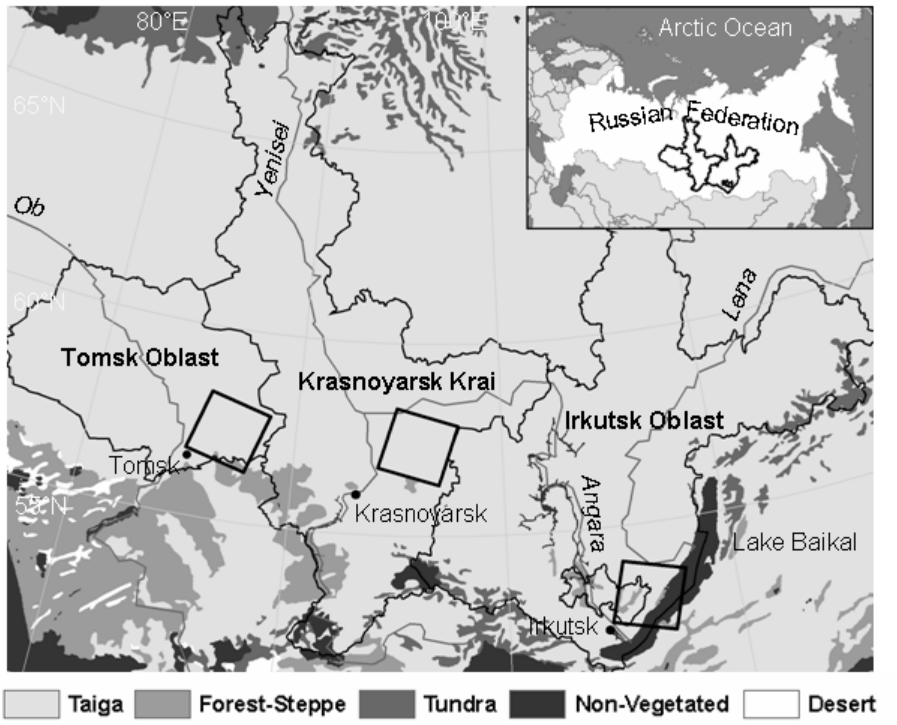

Figure 4.1 Three case study sites (black box outlines) were sampled from Tomsk Oblast, Krasnoyarsk Krai and Irkutsk Oblast (black outline), centered at approximately 57.3°N/86.6°E, 57.3°N/96.1°E and 53.4°N/106.1°E. Source of eco-regions came from Olson *et al.* (2001).

slight gradient from wetter in the west to drier in the east. The dominant ecosystem of the region is boreal taiga, with only minor incursions of temperate-broadleaved and forest-steppe ecosystems (Olson *et al.* 2001). Taiga communities are dominated by tree species of pine, larch, spruce, fir, birch and aspen (Alexeyev and Birdsay 1998). Major forest types are dark-coniferous forest (*Pinus sibirica*, *Picea obovata* and *Abies sibirica*), light-coniferous forest (*Pinus sylvestris* and *Larix sibirica*), broadleaved deciduous forest (*Betula pendula* and *Populus tremula*) and mixed coniferous-deciduous forest.

The characteristic forest disturbances of the study area include logging, fire, and insect infestation. The traditional logging practice of using large landscape-sized clear cuts continued until 1993, after which new regulations established a maximum size of 50 ha for industrial forests. Fires, ranging from small fires at several hectares to large fires at thousands of hectares, are an intrinsic part of boreal forest ecology and in our study region. In our study areas, the Siberian silkmoth (*Dendrolimus sibiricus*) has caused the largest amount of insect damage in recent years. This species primarily attacks mature conifer or mixed coniferous-deciduous forests. During 1993-1996 approximately 0.7 million ha of such forests in Krasnoyarsk Krai were destroyed in silkmoth outbreaks (Kharuk *et al.* 2004). Following logging and fires, young secondary forests, usually dominated by birch and aspen, regenerate and grow on the disturbed sites. An additional factor in regrowing forest patches in this region is now known to be abandonment of collective agriculture fields (Bergen *et al.* 2003).

4.2.2 Data

The land-cover data used for this study were generated from satellite remote sensing for a LCC project that evaluated differences in change regimes prior to and after

the establishment of the Russian Federation in 1991. The data were generated from Landsat MSS (multi-spectral scanner), TM (Thematic Mapper) and ETM+ (Enhanced Thematic Mapper Plus) scenes collected in 1975, 1990 and 2000, respectively. The 30-meter resolution TM and ETM+ data were degraded to 60 meters before classification for use of MSS and TM/ETM+ together. Twelve classes were resolved from these 60-meter Landsat data: Conifer, Mixed, Deciduous and Young forests; Cut, Burn, and Insect disturbances; and Agriculture, Urban, Bare, Wetland and Water. The overall classification accuracies ranged from 89 to 96% (Krankina *et al.* 2005, Bergen *et al.* 2008). For this study, the 1990 and 2000 land-cover datasets were selected for analysis in order to focus on land-cover and biomass changes under current geo-political conditions. All mapped classes were retained for further analysis except Wetland (non-forested) and Water which were excluded given the focus of the study on forest biomass changes and because they remained mostly constant over the study period.

4.3 Methods

4.3.1 Estimating biomass

To understand changes in aboveground standing biomass, a method for assigning appropriate biomass quantities to 60-meter land-cover pixels was required. First, the average biomass density for each land-cover class was estimated using a forest gap model parameterized for Eastern Siberian Forests. Second, the modeled biomass values were assigned to pixels belonging to the corresponding Landsat-derived land-cover classes. In this study, biomass refers to the aboveground standing plant material expressed in Mg C ha^{-1}.

Composition and biomass of forests ranging from young to mature were estimated based on simulation outputs of the FAREAST model, which simulates forest succession and estimates corresponding biomass changes for forests in northeast Eurasia over a range of altitude and climate conditions (Yan and Shugart 2005). FAREAST simulates development of forest stands through the aggregated behavior of individual trees occupying forest plots, each about 0.05 ha in size. The model includes 44 tree species found across northeast Eurasia. It was initially tested for its ability to simulate forest basal area and biomass at different elevations on several tall mountains in Northern China and subsequently validated without recalibration against forest composition registered at 37 sites mostly in Russia and some in China. These sites cover a range of regional climate, soil and elevation conditions.

To apply the FAREAST model to a selected study site, geographic coordinates at the center of the study site were used to base 200 simulations that were then averaged to present latitude, climate and growing season conditions across the site. FAREAST model sites representing multiple forest species compositions in Eastern Siberia were selected to run the simulations, based on their location and/or previously published data on vegetation of the region (Alexeyev and Birdsay 1998, Morozova 2002). The average values of modeled biomass outputs were assigned to each of the categorical Landsat-derived forest types (i.e., Conifer, Mixed, Deciduous and Young). The resulting simulated biomass values for these forest types (Table 4.1) were found to be comparable to the aggregation of documented estimates based on field measurements (e.g., Schulze *et al.* 1999).

The biomass densities of the disturbance and other land-cover classes were estimated based either on extension of the FAREAST-modeled values or previously published literature. Cut or Burn patches identified in the Landsat dataset were likely clear-cut or severely burnt at or shortly before the imaging date, and they were assumed, on average, to be comparable to the initial stage of Young forest with the lowest vegetation recovery rate (Table 4.1). Biomass density for forests affected by insect mortality was assigned based on the assumptions that: 1) defoliation causes an average of 10 Mg ha^{-1} loss of carbon in these Conifer or Mixed forests (Baranchikov *et al.* 2002), 2) dead trees stand 15 years, on average, after being attacked (Pauley *et al.* 1996), and 3) the primary insect attack in the study site took place in 1995 (Kharuk *et al.* 2004). As a result of these assumptions, 2/3 of the aboveground woody biomass (i.e., trunks/branches) was estimated to remain standing in this class by the imaging date in 2000. Biomass density for Agriculture was assigned based on published values in the literature (Shvidenko *et al.* 2000). For Urban and Bare classes (very small categories by area), a biomass value of

Table 4.1 Biomass values assigned to individual land-cover classes

Land Cover	Biomass (Mg C ha^{-1})			Source
	Range		Mean (SD)	
	Min	Max		
Conifer	66.9	134.8	115.4 (14.6)	FAREAST simulation
Mixed	72.9	98.7	92.2 (8.3)	FAREAST simulation
Deciduous	43.9	100.4	74.8 (19.7)	FAREAST simulation
Young	1.9	22.3	12.1 (14.4)	FAREAST simulation
Cut	N/A	N/A	1.9 (N/A)	FAREAST simulation
Burn	N/A	N/A	1.9 (N/A)	FAREAST simulation
Insect	N/A	N/A	62.5 (N/A)	FAREAST simulation, Pauley *et al.* 1996, Baranchikov *et al.* 2002, Kharuk *et al.* 2004
Agriculture	N/A	N/A	4.6 (N/A)	Shvidenko *et al.* 2000
Urban	N/A	N/A	0 (N/A)	N/A
Bare	N/A	N/A	0 (N/A)	N/A

zero was assigned; the mapped Urban category included primarily high-density development with limited vegetation.

4.3.2 Degrading spatial resolution

To estimate Δbiomass at degraded resolutions, the 60-meter land-cover data were aggregated to increasingly coarse resolutions at 240, 480 and 960 meters, roughly analogous to MODIS 250-m, MODIS 500-m, and MODIS/AVHRR 1-km resolutions, respectively. A point spread function (PSF), simulating the larger pixel for these resolutions, was applied in the procedure of resolution degradation. The PSF accounts for the contribution of each location within and nearby a pixel to the detected spectral signal of the pixel (Townshend 1981, Cracknell 1998). It varies with different remote sensing instruments and has been modeled with Gaussian distribution for MODIS and AVHRR sensors (Paithoonwattanakij 1989, Baldwin *et al.* 1998, Huang *et al.* 2002).

Two characteristics of the land-cover data prevented use of the published MODIS and AVHRR PSF to degrade the finer-resolution data. First, the land-cover data were discrete and nominal, as opposed to continuous reflectance values. Second, the original 30-meter Landsat data had been degraded prior to land-cover classification by averaging four neighboring 30-meter Landsat pixels. Therefore, a quasi-PSF was created. This quasi-PSF relied on a 3×3 weighted filter that takes into account information from 60-meter pixels that fell within the degraded pixel and from its eight immediately adjacent pixels. The filter approximates a Gaussian distribution in the two-dimensional space by giving a higher weight (0.68) to the 60-meter pixels within the center degraded pixel and a lower weight (0.04) to those in each of the surrounding eight pixels. The land-cover class of a degraded pixel was determined based on the rank of PSF-weighted averages of

presence counts for individual land-cover categories in all 60-meter pixels within the 3×3 moving window.

4.3.3 Analyzing scale dependence

At each spatial resolution (i.e., 60, 240, 480 or 960 meters), changes between the eleven land-cover classes in 1990 and those in 2000 were assigned a designation of the change category to which they belonged. Theoretically, this could result in 121 possible change directions, but most of these combinations did not occur. In addition, many were functionally similar. Therefore, change directions were grouped into nine meaningful change types (thereafter consistently denoted using Small Caps font to distinguish them from the static land-cover categories):

1. LOGGED: Forest in 1990 cut at or shortly before the 2000 image date, not regenerated or minimally regenerated to forest;
2. BURNED: Forest in 1990 burned at or shortly before the 2000 image date, not regenerated or minimally regenerated to forest;
3. INFESTED: Morality of conifer or mixed forest in 19990 due to insect infestation;
4. DEVELOPED: Forest in 1990 converted to agriculture or urban land in 2000;
5. REGEN I: Forest regeneration after disturbance or from agricultural abandonment occurring between 1990 and 2000 (e.g., Conifer forest in 1990 observed as Young forest regeneration in 2000 due to fire or cut between 1990 and 2000);
6. REGEN II: Young forest regeneration following disturbances or active agriculture identified on the 1990 image;

7. SUCCESSION: Primarily succession of Young in 1990 into Deciduous or Mixed forest types in 2000, also succession of early-successional Deciduous in 1990 to mid-successional Mixed forest in 2000;
8. CONSTANT: Areas of no change between 1990 and 2000;
9. UNKNOWN: Any change not listed above (likely classification error).

Changes in biomass at each spatial resolution were estimated by 1) deriving biomass values for each pixel based on its land-cover types in 1990 and 2000, respectively, 2) calculating differences between biomass values in the two years for each pixel, and 3) pooling these biomass changes by the nine LCC types.

The scale dependence of the estimated changes in land cover and biomass was analyzed at the increasingly coarser resolutions using the 60-meter LCC and Δbiomass as reference. Scale dependence was defined as the measure of agreement or disagreement of an estimate derived at a coarse resolution to the same estimate at the reference resolution. Lower agreement (or higher disagreement) is associated with greater scale dependence. With respect to changes in land cover, scale dependence was examined using the error matrix method, with land-cover changes identified at the coarse resolution analogous to 'classified' data and corresponding changes at the 60-meter resolution analogous to 'reference' data in a conventional error matrix (Congalton and Green 1999). The scale dependence of Δbiomass was examined based on the root mean squared error (RMSE) between Δbiomass quantities calculated at the 60-meter and coarser resolutions. For these analyses, pixels at coarser resolutions were resampled to 60 meters. Lower accuracies or higher RMSE indicate lower agreement of the identified LCC and calculated Δbiomass, and hence higher scale dependence.

4.3.4 Analyzing patch characteristics

We analyzed land-cover patch characteristics to evaluate the effects of patch sizes of characteristic disturbances in Eastern Siberian forests on uncertainties of the estimated Δbiomass at different remote sensor resolutions. Instead of focusing on the spatial arrangement of land-cover classes at individual imaging dates, we investigated patch characteristics of different types of land-cover changes observed from the two imaging dates.

At the 60-meter resolution, mean patch size (MPS), edge density (ED) and mean shape index (MSI) were calculated for each LCC type in each case study site using ArcView GIS Patch Analyst extension (McGarigal and Marks 1995, Rempel 2006). The relationships between these landscape indices at 60 meters and RMSE of Δbiomass at 960 meters were then analyzed using three different generalized linear regression models (GLM), one for each landscape pattern index. The GLM independent variable was the pixel-wise RMSE of the estimated Δbiomass averaged by LCC types for each of the three sites at 960 meters. The GLM predictors included one of the three patch indices at 60 meters for each model and also a site indicator to test for differences among sites. There were 24 observations in each of the regression models, corresponding to the seven, nine, and eight existing LCC types for Tomsk, Krasnoyarsk, and Irkutsk sites, respectively.

4.4 Results

4.4.1 Changes in land cover and biomass at 60-meter resolution

The nine LCC types were divided into four groups, including Forest Disturbance, Forest Regrowth, Constant, and Unknown (Table 4.2). Forest Disturbance is defined as any land-cover change resulting in the net loss of forest biomass. This includes the

Table 4.2 Changes in land cover (%) and biomass (Mg C ha^{-1}) at the 60-meter resolution. The *subtotal* and *total* is the sum of Δbiomass weighted by proportions of area occupied by individual land-cover change types.

Land-Cover Change	**Tomsk**			**Krasnoyarsk**			**Irkutsk**		
	% by area	ΔBiomass	Area-weighted ΔBiomass	% by area	ΔBiomass	Area-weighted ΔBiomass	% by area	ΔBiomass	Area-weighted ΔBiomass
Forest Disturbance									
LOGGED	1.48	-82.14	-1.22	1.15	-64.44	-0.74	0.50	-95.83	-0.48
BURNED	0.00	0.00	0.00	0.66	-56.36	-0.37	2.49	-96.13	-2.39
INFESTED	0.00	0.00	0.00	6.20	-30.20	-1.87	0.00	0.00	0.00
DEVELOPED	0.58	-44.19	-0.25	1.96	-44.57	-0.88	0.48	-85.93	-0.41
REGEN I	2.83	-69.92	-1.98	1.40	-80.11	-1.12	0.51	-60.03	-0.31
Subtotal			***-3.45***			***-4.98***			***-3.59***
Forest Regrowth									
REGEN II	6.09	28.93	1.76	3.74	33.63	1.25	2.15	58.41	1.26
SUCCESSION	9.16	51.28	4.70	17.17	58.83	10.10	6.85	27.04	1.85
Subtotal			***6.46***			***11.35***			***3.11***
Unknown	4.52	-7.42	***-0.34***	6.97	4.96	***0.34***	12.76	-14.62	***-1.87***
Constant	75.35	0.00	***0.00***	60.75	0.00	***0.00***	74.26	0.00	***0.00***
Total*			***+3.01***			***+6.37***			***-0.48***

* Excludes the Unknown and Constant types.

LOGGED, BURNED, INFESTED, DEVELOPED and REGEN I (i.e., forest that is regenerating but still represents a net loss of biomass due to interim disturbance events) types. Forest Regrowth refers to land-cover changes between 1990 and 2000 associated with net gains in forest biomass. This includes the REGEN II and SUCCESSION types.

During the time period between 1990 and 2000, approximately 20, 32, and 13% of the total area in the Tomsk, Krasnoyarsk and Irkutsk sites experienced changes in land-cover type (Table 4.2). In the Forest Disturbance group, a greater amount of LOGGED area was directly observed in the Tomsk and Krasnoyarsk sites and a somewhat lesser amount in the Irkutsk site. The largest proportion of very recent burn scars (i.e., BURNED) was detected in the Irkutsk site (2.5%). Only the Krasnoyarsk site was associated with INFESTED during the study period. All three sites had a small amount of DEVELOPED. Interim disturbances (i.e., REGEN I) also occurred in all three sites, with the slightly greater proportion in Tomsk and Krasnoyarsk sites and slightly less in the Irkutsk site. In the Forest Regrowth group, REGEN II (Cut, Burn or Agriculture in 1990 and Young or Deciduous in 2000) was present on 2-6% of the total land area with greater proportions in the Tomsk and Krasnoyarsk sites than in the Irkutsk site. For all three case study sites, a somewhat greater proportion of SUCCESSION was found.

Among the Forest Disturbance categories, the LOGGED and BURNED types were associated with the highest biomass loss per unit area (Table 4.2), as together they represented primarily high biomass forests in 1990 converted to negligible biomass Cut or Burn in 2000. Similarly, REGEN I (interim disturbances) resulted in a high loss of biomass across all three case study sites, with relatively small biomass recovery as Young forest at the 2000 date. Of categories in the Forest Disturbance group, INFESTED caused

the least reduction of biomass per unit area, because of the biomass retained in the still standing tree stems even after defoliation and mortality. Compared to the biomass loss in the Forest Disturbance group, the biomass gained per unit area over ten years for LCC types within the Forest Regrowth group was much smaller on average. However, since the amount of area in the Forest Regrowth group was two to three times larger than the area of the Forest Disturbance group, the total biomass increment in a site due to regeneration and succession exceeded biomass loss due to disturbances and development (Tomsk and Krasnoyarsk sites) except where large-extent severe burns took place (Irkutsk site). Forest Regrowth occupied a larger area, because it includes not only forest patches regenerating from the disturbed land in 1990 but also patches that were disturbed prior to 1990 and underwent succession, plus patches of abandoned agriculture undergoing land-cover conversion to forest types. At the site level, the average Δbiomass (excluding the Unknown or Constant types) was estimated to be 3.01, 6.37 and -0.48 Mg C ha^{-1} for the Tomsk, Krasnoyarsk and Irkutsk sites, respectively.

4.4.2 Scaling effects

For all three sites, the CONSTANT LCC type retained a high accuracy relatively to the 60-meter reference (Figure 4.2) and, therefore, its scale dependence was low. The LOGGED and DEVELOPED types had consistently low accuracy at the degraded resolutions; therefore, their scale dependence was high. Producer's accuracy of the BURNED type declined faster in the Krasnoyarsk site (Figure 4.2D) and slower in the Irkutsk site (Figure 4.2F), indicating a reduced scale dependence in the Irkutsk site. The two regeneration and successional types were also scale-dependent. In the Tomsk and

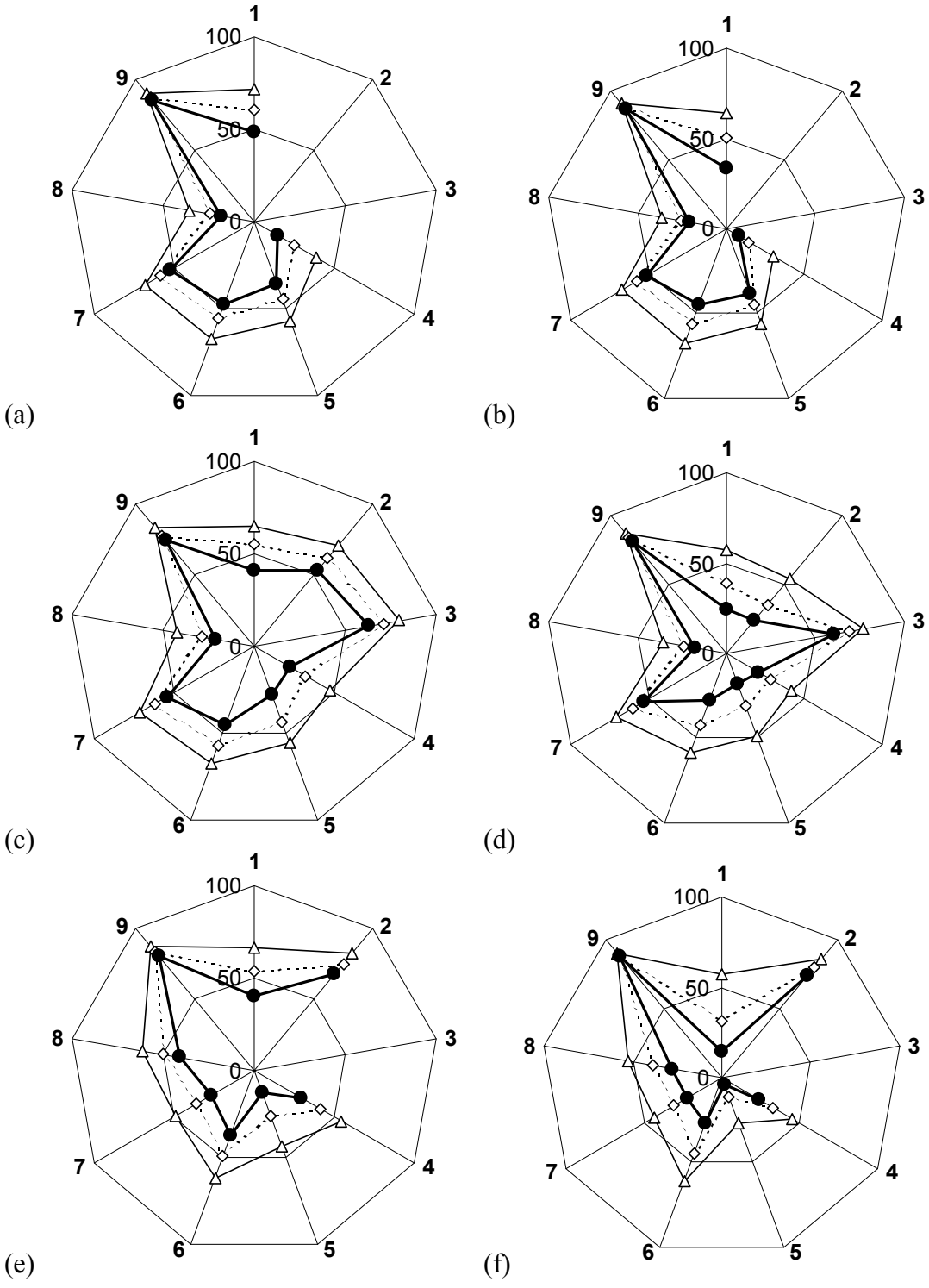

Figure 4.2 User's and Producer's accuracy of the degraded land-cover change at the 240- (triangle), 480- (square) and 960-meter (solid circle) resolution for the Tomsk (a, b), Krasnoyarsk (c, d) and Irkutsk (e, f) sites. The reference is the 60-meter land-cover change dataset. Land-cover change codes are: 1 LOGGED, 2 BURNED, 3 INFESTED, 4 DEVELOPED, 5 REGEN I, 6 REGEN II, 7 SUCCESSION, 8 UNKNOWN, and 9 CONSTANT.

Krasnoyarsk sites REGEN I appeared to be more scale-dependent than REGEN II or SUCCESSION, but all three types showed a higher sensitivity to scale in the Irkutsk site.

Overall accuracies (i.e., indicators of scale dependence) of the detected land-cover changes at the 960-meter resolution vs. the 60-meter reference were 74.9%, 65.4% and 72.8% for the Tomsk, Krasnoyarsk and Irkutsk sites, respectively. Given that the overall accuracies of land-cover classifications were 89-96% at the 60-meter resolution, the accuracies of land-cover changes were estimated to range between 79 and 92% at this resolution (Bergen *et al.* 2008). Therefore, on the basis of this scale dependency analysis, accuracies of the identified land-cover changes at the 960-meter resolution may vary between 52% (i.e., 0.79×0.654) and 69% (i.e., 0.92×0.749). This indicates that, based on the simulated land-cover data, scale dependence may cause a drop of approximately 20-30% in accuracy of the detectable land-cover changes between the 60- and 960-meter resolutions.

Across the three sites, the LOGGED and DEVELOPED types were highly scale-dependent and, therefore, their areas were not retained well at the degraded resolutions (Figure 4.3A-C). BURNED was also highly scale-dependent in the Krasnoyarsk site and, therefore, was considerably underestimated at coarser resolutions (Figure 4.3B). However, BURNED was less dependent on scales in the Irkutsk site where it was overestimated at coarse resolutions (Figure 4.3C). INFESTED in the Krasnoyarsk site had an intermediate level of scale dependence and was slightly under-represented at the degraded resolutions (Figure 4.3B). Most of the remaining dynamic LCC types were underestimated, in contrast to the CONSTANT type, which was always overestimated (Table 4.3). The rate of

overall under-estimation of Forest Disturbance types exceeded that of the Forest Regrowth types.

With respect to Δbiomass between 1990 and 2000, the site-level estimates at the 960-meter resolution were 3.30, 6.97 and -0.83 Mg C ha^{-1} for the Tomsk, Krasnoyarsk and Irkutsk sites, respectively. These were equivalent to differences of 9.6, 9.4 and 69.4%, compared to the Δbiomass quantities calculated at the 60-meter resolution. For all three sites, the magnitude (absolute value) of the estimated Δbiomass increased with

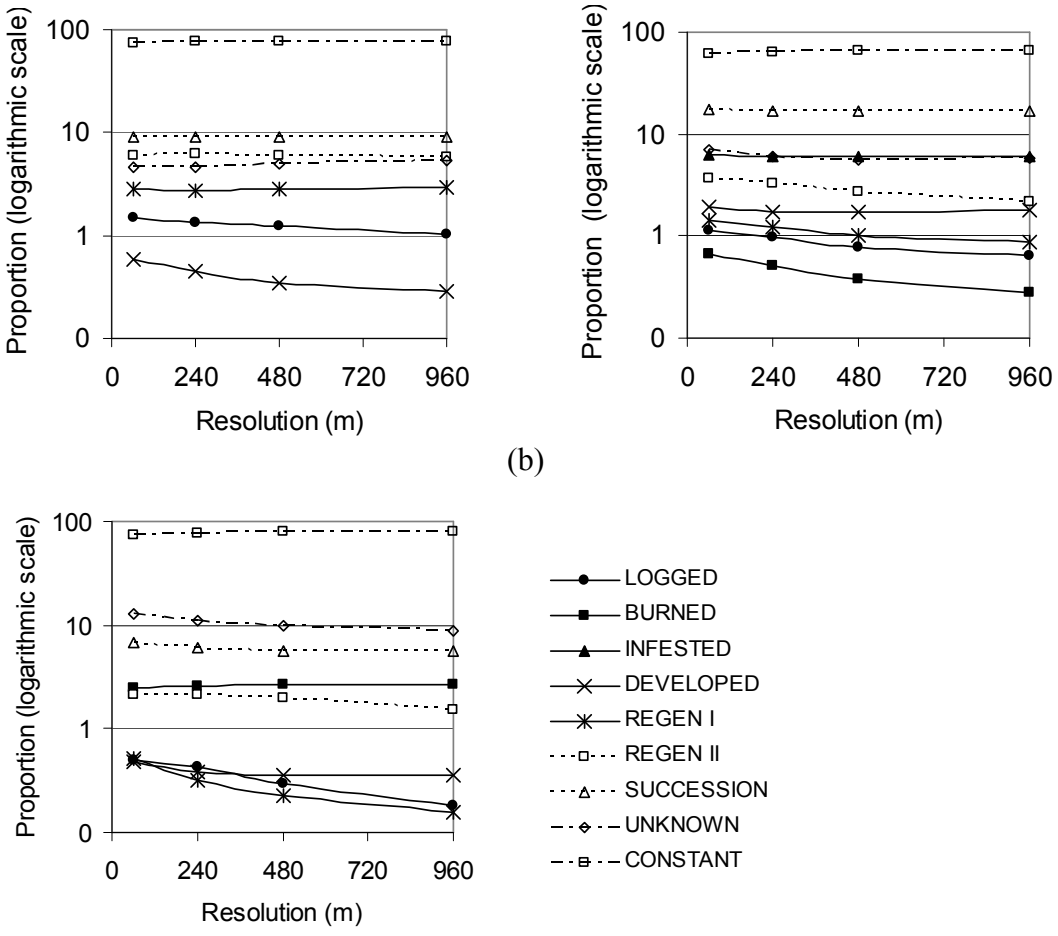

Figure 4.3 Proportion of individual land-cover changes identified at the degraded spatial resolutions in the Tomsk (a), Krasnoyarsk (b) and Irkutsk (c) sites.

Table 4.3 Proportions of land-cover change types at 60- and 960-meter resolutions. Their differences in proportion with respect to their 60-m proportion are shown in bold numbers, where negative values indicate under-estimation of area at the 960-meter resolution and positive values over-estimation.

Land-Cover	**Tomsk**			**Krasnoyarsk**			**Irkutsk**		
Change	**60-m**	**960-m**	**Diff. (%)**	**60-m**	**960-m**	**Diff. (%)**	**60-m**	**960-m**	**Diff. (%)**
LOGGED	1.48	1.02	**-30.92**	1.15	0.65	**-43.27**	0.50	0.18	**-64.27**
BURNED	0.00	0.00	**N/A**	0.66	0.28	**-57.14**	2.49	2.71	**8.61**
INFESTED	0.00	0.00	**N/A**	6.20	6.06	**-2.36**	0.00	0.00	**N/A**
DEVELOPED	0.58	0.29	**-51.15**	1.96	1.81	**-7.49**	0.48	0.36	**-25.38**
REGEN I	2.38	2.89	**2.03**	1.40	0.88	**-37.56**	0.51	0.16	**-69.95**
REGEN II	6.09	6.68	**-6.61**	3.74	2.19	**-41.51**	2.15	1.53	**-29.00**
SUCCESSION	9.16	9.05	**-1.19**	17.17	16.65	**-3.02**	6.85	5.63	**-17.81**
UNKNOWN	4.52	5.26	**16.49**	6.97	5.71	**-18.19**	12.76	13.50	**5.80**
CONSTANT	75.35	75.81	**0.62**	60.75	65.78	**8.28**	74.26	75.95	**2.27**

degradation of spatial resolutions (Figure 4.4A). The same trend was found for the pixel-level RMSE for the estimated Δbiomass (Figure 4.4B). At the 960-meter resolution, RMSE was 21.38, 30.22 and 32.12 Mg C ha^{-1} in the Tomsk, Krasnoyarsk and Irkutsk sites, respectively. This, on average, is equivalent to up to 28% of the pixel-level maximum potential biomass change (Table 4.1) in the study area during 1990-2000.

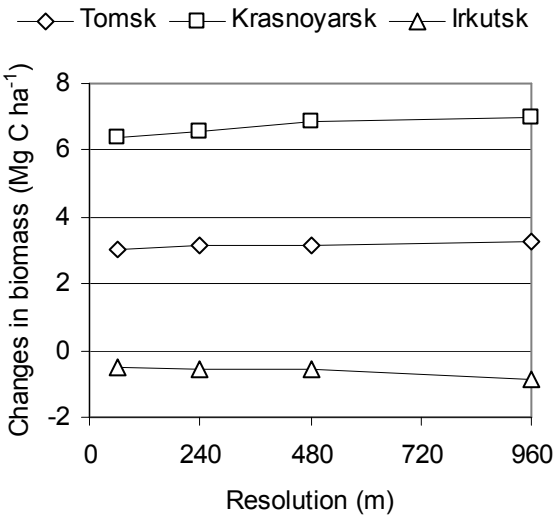

(a)

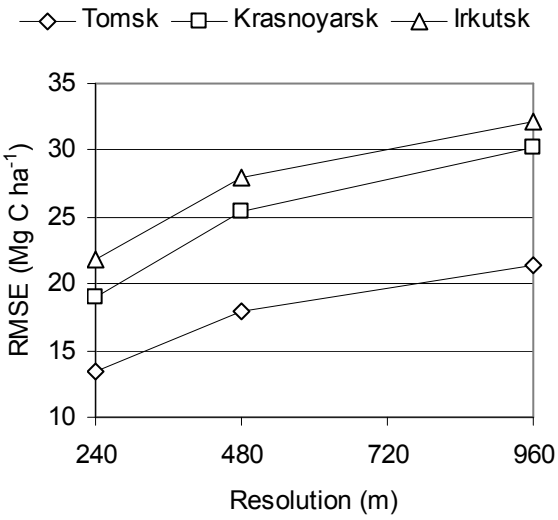

(b)

Figure 4.4 Estimated Δbiomass (Mg C ha^{-1}) at 60-meter and degraded resolutions (a) and its RMSE with the 60-meter estimates at degraded resolutions (b).

4.4.3 Spatial characteristics of the land-cover changes

The mean patch size (MPS), edge density (ED) and mean shape index (MSI) varied by different LCC types across the three case study sites at the 60-meter resolution (Figure 4.5). Across the three sites, LOGGED had a relatively consistent MPS (4.2-5.5 ha)

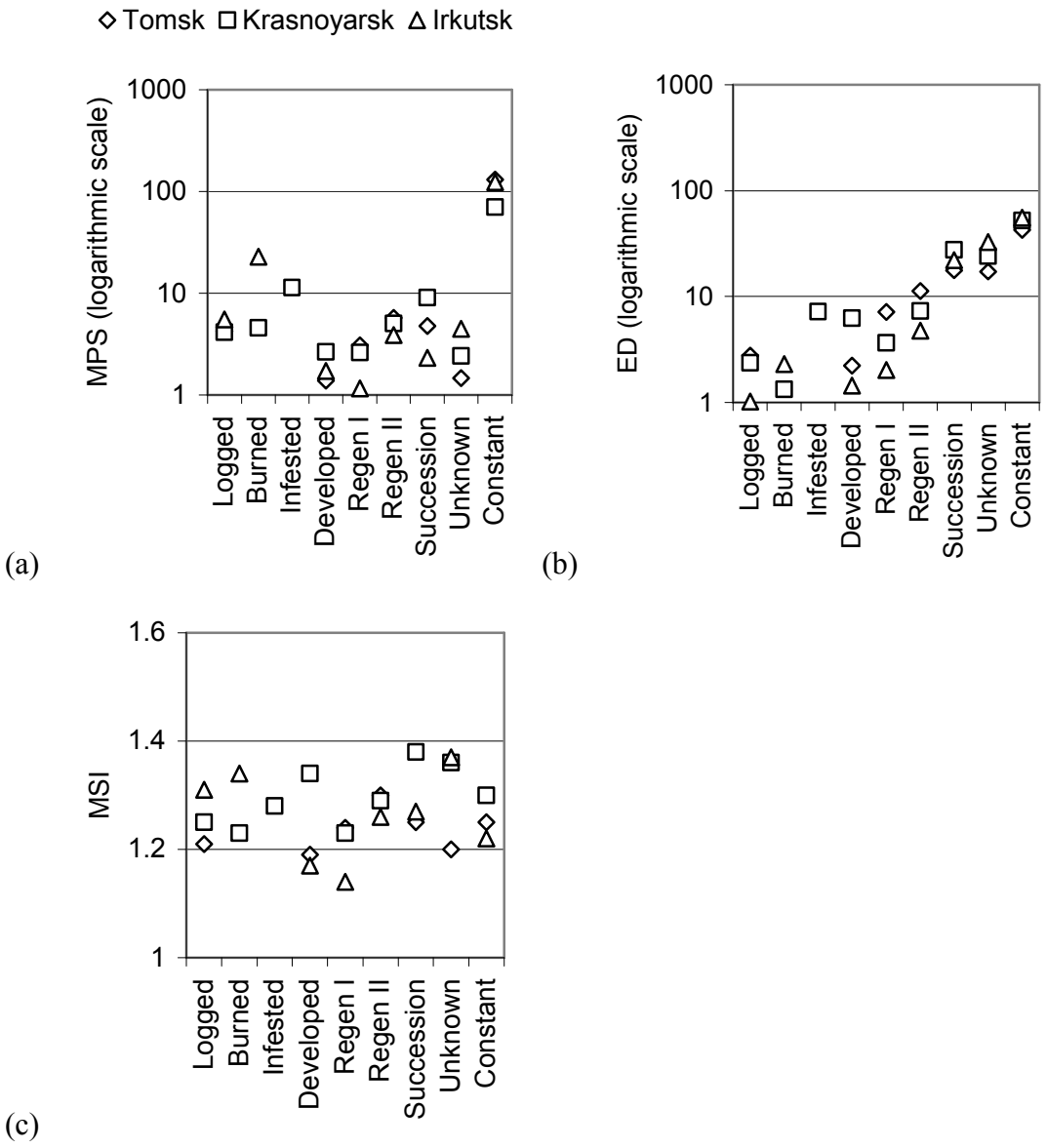

Figure 4.5 Mean patch size (a), edge density (b), and mean shape index (c) of three case study sites.

and somewhat variable edge and shape characteristics. Spatial characteristics of BURNED varied across sites, including: 1) no burns could be conclusively identified in the Tomsk site during the time period of 1990-2000; 2) new burn scars were small on average (4.6 ha) in the Krasnoyarsk site, but large (23 ha) in the Irkutsk site; and 3) the shape of BURNED patches was more complex in the Irkutsk site (1.34) than in Krasnoyarsk (1.23). The MPS of INFESTED patches was relatively large in the Krasnoyarsk site (the only site in which this type occurred; 11 ha), with intermediate MSI (1.28). For REGEN I or II patches, MPS and MSI were found similar in the Tomsk and Krasnoyarsk site, but different in the Irkutsk site which has more complex terrain.

The relationships between RMSE of the estimated Δbiomass at 960 meters and the three LCC patch indices at 60 meters, based on regression models, showed that MPS and ED were significant ($p \leq 0.001$) predictors for RMSE of Δbiomass and that MSI was not a significant predictor (Table 4.4). The higher the MPS, the lower the RMSE, given that, if the landscape were continuous, estimates of changes in biomass at the 960-meter resolution would converge on estimates produced at the 60-meter resolution. ED was also significantly negatively related to RMSE, which means that the scale dependence of the estimated Δbiomass was high for LCC types with low edge densities. The site predictor was not significant, based on regression models (Table 4.4). This implied that relationships between RMSE and patch indices were consistent across the three sites, indicating the general scaling impacts on errors of the estimated Δbiomass rather than specific spatial characteristics of a site.

Table 4.4 Regression model results for the relationship between RMSE of the estimated Δbiomass at 960 meters and patch metrics of individual LCC types at 60 meters. The pixel-wise RMSE was pooled by LCC types at each case study site. In all three models, RMSE is the dependent variable. Independent variables include patch indices and site indicator. The adjusted R square is the indicator of model fit.

GLM	Adjusted R square	Source	Type III sum of squares	df*	Mean square	F	Sig.
1	0.411	Corrected model	3355.732	3	1118.577	6.341	0.003
		Intercept	56305.828	1	56305.828	319.163	0.000
		MPS	2803.725	1	2803.725	15.893	0.001
		Site	730.954	2	365.477	2.072	0.152
		Error	3528.342	20	176.417		
		Total	64820.782	24			
		Corrected Total	6884.073	23			
2	0.528	Corrected model	4058.132	3	1352.711	9.574	0.000
		Intercept	47130.159	1	47130.159	333.554	0.000
		ED	3506.126	1	3506.126	24.814	0.000
		Site	610.796	2	305.398	2.161	0.141
		Error	2825.941	20	141.297		
		Total	64820.782	24			
		Corrected Total	6884.073	23			
3	-0.030	Corrected model	719.823	3	239.941	0.778	0.520
		Intercept	572.853	1	572.853	1.859	0.188
		MSI	167.816	1	167.816	0.544	0.469
		Site	544.646	2	272.323	0.884	0.429
		Error	6164.250	20	308.213		
		Total	64820.782	24			
		Corrected Total	6884.073	23			

* Degree of freedom

4.5 Discussion

The carbon landscape of Eastern Siberia is a dynamic one driven by forest disturbances as indicated by these results and corroborated by regional studies. For example, in the southern part of Krasnoyarsk Krai, studies have shown that disturbance over the past century has affected 62-85% of forests in that region (Sokolova 2000). Whereas a large proportion of the regional forest up through the 19th century was comprised of mature dark coniferous forest, the late 20th century forest of the present

study is dominated by light-coniferous, mixed or young deciduous forest types, generally at early- to mid-successional stages (Hytteborn *et al.* 2005; Bergen *et al.* 2008). These trends illustrate the overarching importance of forest disturbance and regrowth associated with logging, fire, and insect characteristic of the region.

4.5.1 Changes in forest type and biomass due to land-cover change

Our estimates based on land-cover changes showed that biomass due to forest disturbance and regrowth increased 3-6 Mg C ha^{-1} in the Tomsk and Krasnoyarsk sites and declined 0.5 Mg C ha^{-1} in the Irkutsk site between 1990 and 2000. The slight decline in the Irkutsk site was due mainly to its extensive and severe fires, identified as fresh brun scars in the 2000 Landsat, which were not present or minimal at the Tomsk and Krasnoyarsk sites at the same date. Other studies that have mapped fires in the region corroborate this spatial and temporal distribution of light to severe fire regimes during the same time period (e.g., George *et al.* 2006).

The increase of biomass in the Tomsk and Krasnoyarsk sites resulted from biomass gained through forest regrowth (regeneration and succession combined), which exceeded biomass lost through forest disturbance. Although areas of regrowth had generally smaller biomass increments per unit area than those lost due to disturbance, during the study period the area of the regrowth was larger. The area of the REGEN II category was large due to the fact that this included regeneration of Young forest on former agricultural lands. The large area of SUCCESSION was a result of earlier fire and logging disturbances prior to the study period. Fire has always been a disturbance factor across the study area, and Krasnoyarsk and Tomsk in particular were the sites of large

landscape-sized clear cuts prior to the 1990s. The average Δbiomass was 3.9 Mg C ha^{-1} pooled by the three study sites.

While the land-cover data were of reasonable accuracy (overall accuracy ranging from 89-96%; Bergen *et al.* 2008), forest type classification errors are one of the uncertainties associated with estimates of Δbiomass for this study. In the Tomsk and Krasnoyarsk sites, all forest types had the highest accuracy of the land-cover classes. In the Irkutsk site, however, classification accuracies of the Mixed, Deciduous and Young forest types were relatively lower in both 1990 and 2000 (accuracies ranged from 0.71 to 0.90 with an average of 0.81). This indicates some classification confusion between young and maturing forest stands, which might have introduced bias in the calculated proportions of regeneration and succession types in the Irkutsk site.

Areas that did not change land-cover types between 1990 and 2000 were held constant in terms of biomass for the current study. However, in a more complete accounting of carbon, biomass changes within a particular successional stage due to growth and respiration would also be considered. As noted, wetlands were excluded from this study because of little confirmed conversion between wetlands and forested land-cover classes in the study area between 1990 and 2000 as well as the large discrepancy of documented carbon values for wetlands (Arneth *et al.* 2002, Smith *et al.* 2004). However, their roles as sinks or sources of carbon dioxide are potentially important, though the magnitude is debated.

4.5.2 Scaling and amplified estimates at MODIS/AVHRR resolutions

Remote sensing data collected with the coarse-resolution sensors such as AVHRR, MODIS and SPOT VEGETATION have been employed widely in the monitoring of

forest and biomass changes at regional to global scales. These sensors are advantageous in their large swath dimension and frequent repeat cycle, which make it possible to obtain cost-effective, instantaneous and cloud-minimized data for the large and often remote forested regions such as Siberia. However, a major concern in Siberia and elsewhere is whether the ability of the sensors to detect change is constrained by their limited spatial resolution with respect to characteristic land-cover and disturbance patch sizes. For example, a study of the tropical fire database showed that fast-repeating coarse-resolution sensors had advantages of capturing many active fires (including those burned out rapidly because of low fuel load) at the expense of missing a large number of small fires (Bradley and Millington 2006). A study in the Russian Federation documented that over one-third of burn scars were smaller than 2 km^2 and that failure to record these small burn scars in the multi-temporal SPOT VEGETATION dataset resulted in a 10% reduction of the estimated carbon emission from fires (Zhang *et al.* 2003).

We found more complex results based on scaling of the Landsat LCC data in our study area. Among all LCC types, CONSTANT (i.e., the unchanged area) was consistently less scale-dependent but was over-represented at the degraded spatial resolutions due to its large average patch size. All types in the Forest Disturbance group except for a few cases of BURNED and likely fire-related REGEN I patches were dependent on scale and were underestimated at the 960-meter resolution (Table 4.3). Fire scars in one case study site (Krasnoyarsk) were relatively small in size (4.6 ha on average); therefore, >50% of these fires disappeared at the 960-meter resolution. On the contrary, fire scars in the Irkutsk site were large in size (23 ha), which resulted in an over-estimation of the burned area by about 9% at the 960-meter resolution. Patches of LOGGED and DEVELOPED were

generally somewhat smaller in size (<5.5 ha on average) than INFESTED (11 ha on average); therefore, the proportion of the identifiable patches declined at a greater rate for the LOGGED and DEVELOPED types than for the INFESTED type, when LCC data were progressively degraded. All categories in the Forest Regrowth group were underestimated at the 960-meter resolution, but at a smaller rate compared to the Forest Disturbance group.

In summary, although all of the LCC types as a whole tended to be underestimated at the MODIS and AVHRR resolutions, Forest Regrowth types and the large-sized Forest Disturbance types (such as INFESTED and large BURNED patches) retained presence better than the small-sized disturbances (such as the DEVELOPED, LOGGED and small BURNED patches). In turn, the lost information on small disturbances or development contributed to the overestimated biomass accumulation at the 960-meter resolution in the Tomsk and Krasnoyarsk sites. The over-represented BURNED areas contributed to the overestimated biomass decline at the 960-meter resolution in the Irkutsk site. This implies that, at the degraded spatial resolution, information on disturbances may be under- or over-estimated depending on their average patch sizes. Consequently, the estimated value of changes in biomass at the coarse resolutions may be amplified regardless of the change directions.

At the site level, uncertainties in the estimated Δbiomass by different LCC types had a significant correlation with the MPS and ED of these LCC types (Table 4.4). Low uncertainties were associated with large-sized land-cover changes (i.e., high MPS values), indicating that large-sized changes were less prone to errors of identification at degraded resolutions. However, the results showed that simple patch edges were clearly associated

with high uncertainties of the estimated Δbiomass, while the complex patch edges were associated with low uncertainties. LOGGED in the study sites was typically regular in shape with simple edges, stemming from logging regulations on industrial forest lands. High uncertainties of the estimated Δbiomass of logging occurred at the coarse spatial resolution was not because of its simple edges, though they were well correlated, but because of the loss of logging due to its small patch sizes.

This analysis specifically quantifies scaling effects of sensor resolution on estimated changes in land cover and biomass. Although not intended to simulate real MODIS/AVHRR sensor data, the results of this study have implications for uncertainties related to the large-area monitoring of biomass changes using sensors with resolutions like those of MODIS/AVHRR. However, there are two noted limitations of this study for drawing direct conclusions about the usefulness of these specific sensors. First, the simulated point spread function (PSF) was used for estimation of coarse image pixels. Such simulation of a coarse pixel, although taking into account distribution of signals at different locations, was not identical to the PSF of the MODIS/AVHRR sensors. Second, spectral information of the Landsat and MODIS/AVHRR sensors is also different, which might introduce different interpretations of land cover using the scaled Landsat vs. remotely sensed MODIS/AVHRR data.

4.6 Conclusions

We investigated biomass changes due to disturbance and regrowth in three case study sites representative of Eastern Siberia, and analyzed the implications of remote sensing spatial resolution on the estimated LCC proportions and Δbiomass resulting from characteristic forest dynamics of this region.

During the time period 1990-2000, up to one-third of the total land area within the three sites experienced land-cover changes associated with forest disturbances (logging, fire, insect infestation and development) and recovery of natural vegetation (including regeneration and succession). Biomass of the Tomsk and Krasnoyarsk sites was estimated to increase in 2000, while that of the fire-prone Irkutsk site showed a slight decline during the same time period. The increase of biomass was mainly due to natural regeneration and succession following historical and contemporary forest disturbances and agriculture abandonment. The negligible decrease for Irkutsk was likely due to a severe fire year in the 2000 end-point Irkutsk scene, where vegetation had not had a chance to regrow. Since biomass accumulation results from the net carbon uptake of vegetation, the overall increase in biomass implies that, collectively, the aboveground vegetation in the three sampled sites accumulated carbon because of land-cover changes between 1990 and 2000. Without information about carbon exchange in soils, however, it is impossible to say whether these landscapes were net carbon sources or sinks.

These data were used to examine the impact of resolution of remote sensing data on estimates of Δbiomass. Aggregating from 60 to 960 meters, information lost due to the coarsened image resolution was consistently greater for the disturbance types combined than for the regrowth types combined. Therefore, in most cases there is an over-estimation of biomass gain at the degraded spatial resolutions (Figure 4.4A). In areas with extensive and continuous fires, over-estimation of biomass loss tends to occur due to the over-recorded fire pixels at the coarse resolution (Figure 4.4A). The sizes of disturbance patches (especially fires that have wide ranges of sizes) play an important role in the carbon estimation based on coarse-resolution remote sensing data. With

respect to uncertainties of the estimated Δbiomass, the average pixel-wise RMSE increased significantly with the degraded resolution from 60 to 960 meters (Figure 4.4B).

A rationale for undertaking this study is the concern that estimation based on >250 meter satellite data may be biased due to the lost spatial details relative to patch sizes of land cover and land-cover dynamics in Siberia. The results illustrate the spatial characteristics of disturbance and regrowth patch in representative Siberian forests, and the differences in Δbiomass estimated using coarser resolution remote sensing data. With caveats related to differences in the spectral and point-spread characteristics of sensors, these results can be used to inform selection of remotely sensed data based on spatial resolutions and in interpretation of uncertainties associated with the widely used MODIS/AVHRR land-cover and biomass data for Siberian Forests.

References

Alexeyev, V.A. and Birdsay, R.A., 1998, Carbon storage in forests and peatlands of Russia. USDA Forest Service. General Technical Report NE-244.

Aplin, P., 2006, On scales and dynamics in observing the environment. *International Journal of Remote Sensing*, 27 (11), 2123-2140

Arneth, A., Kurbatova, J., Kolle, O., Shibistova, O.B., Lloyd, J. and others, 2002, Comparative ecosystem-atmosphere exchange of energy and mass in a European Russia and a central Sibeiran bog II: Interseasonal and interannual variability of CO2 fluxes. *Tellus*, 54B, 514-530.

Asner, G.P., Keller, M., Pereira, R. and Zweede, J.C., 2002, Remote sensing of selective logging in Amozonia: Assessing limitations based on detailed field observations, Landsat ETM+, and textural analysis. *Remote Sensing of Environment*, 80, 483-496.

Atkinson, P.M. and Curran, P.J., 1997, Choosing an appropriate spatial resolution for remote sensing investigations. *Photogrammetric Engineering & Remote Sensing*, 63, 1345-1351.

Baldwin, D.G., Emery, W.J. and Cheeseman, P.B., 1998, Higher resolution Earth surface features from repeat moderate resolution satellite imagery. *IEEE Transactions on Geoscience and Remote Sensing*, 36 (1), 244-255.

Baranchikov, Yu.N., Perevoznikova, V.D. and Vishnyakova, Z.V., 2002, Carbon emission by soils in forests damaged by the Siberian moth. *Russian Journal of Ecology*, 33 (6), 398-401.

Bartalev, S.A., Belward, A.S., Erchov, D.V. and Isaev, A.S., 2003, A new SPOT4-VEGETATION derived land cover map of Northern Eurasia. *International Journal of Remote Sensing*, 24(9), 1977-1982.

Bergen, K.M., Conard, S.G., Houghton, R.A., Kasischke, E.S., Kharuk, V.I. and others, 2003, NASA and Russian scientists observe land-cover and land-use change and carbon in Russian forests. *Journal of Forestry*, 101 (4), 34-41.

Bergen, K.M., Zhao, T., Kharuk, V., Blam, Y., Brown, D.G., 2008, Changing regimes: Forested land-cover dynamics in Central Siberia 1974-2001. *Photogrammetric Engineering & Remote Sensing* (forthcoming).

Bradley, A.V. and Millington, A.C., 2006, Spatial and temporal scale issues in determining biomass burning regimes in Bolivia and Peru. *International Journal of Remote Sensing*, 27 (11), 2221-2253

Caylor, K.K. and Shugart, H.H., 2004, Simulated productivity of heterogeneous patches in Southern African savanna landscapes using a productivity model. *Landscape Ecology*, 19, 401-415.

Congalton, R.G. and Green, K., 1999, Assessing the Accuracy of Remotely Sensed Data: Principles and Practices. Boca Raton, FL: Lewis Publishers.

Cracknell, A.P., 1998, Synergy in remote sensing – what's in a pixel? International Journal of Remote Sensing, 19 (11), 2025-2047.

Food and Agriculture Organization of the United Nations, 2005, State of the World's Forests. Available online at: http://www.fao.org/docrep/007/y5574e/y5574e00.HTM (accessed 2 March 2007)

George, C., Rowland, C., Gerard, F. and Balzter, H., 2006, Retrospective mapping of burnt areas in Central Siberia using a modification of the normalized difference water index. *Remote Sensing of Environment*, 104, 346-359.

Huang, C., Townshend, J.R.G., Liang, S., Kalluri, N.V. and DeFries, R.S., 2002, Impact of sensor's point spread function on land cover characterization: assessment and deconvolution. *Remote Sensing of Environment*, 80, 203-212.

Hytteborn, H., Maslov, A.A., Nazimova D.I. and Rysin, L.P., 2005, Boreal Forests of Eurasia. In *Ecosystems of the World: Coniferous Forests*, F. Anderssen (Ed.) (Elsevier, Amsterdam), pp. 23-99.

Kharuk, V.I., Ranson, K.J., Burenina, T.A. and Fedotova, E.V., 2003, Mapping of Siberian forest landscapes along the Yenisey transact with AVHRR. *International Journal of Remote Sensing*, 24 (1), 23-37.

Kharuk, V.I., Ranson, K.J., Kozuhovskaya, A.G., Kondakov, Y.P. and Pestunov, I.A., 2004, NOAA/AVHRR satellite detection of Siberian silkmoth outbreaks in eastern Siberia. *International Journal of Remote Sensing*, 25 (24), 5543-5555.

Krankina, O., Sun, G., Shugart, H.H., Kasischke, E., Kharuk, V.I., Bergen, K.M., Masek, J.G., Cohen, W.B., Oetter, D.R. and Duane, M.V, 2005, Northern Eurasia: Remote sensing of boreal forest in selected regions, *Land Change Science: Observing, Monitoring, and Understanding Trajectories of Change on the Earth's Surface*, Kluwer, Dordrecht, Netherlands, pp. 123-138.

Lloyd, J., Shibistova, O., Zolotoukhine, D., Kolle, O., Arneth, A. and others, 2002, Seasonal and annual variations in the photosynthetic productivity and carbon balance of a central Siberian pine forest. *Tellus*, 54B, 590-610.

Mayer, A.L., Kauppi, P.E., Angelstam, P.K., Zhang, Y. and Tikka, P.M., 2005, Importing timber, exporting ecological impact. *Science*, 308, 359-360.

McGarigal, K. and Marks, B.J., 1995, FRAGSTATS: spatial pattern analysis program for quantifying landscape structure. USDA For. Serv. Gen. Tech. Rep. PNW-351.

Morozova, O., 2002, Vegetation. In: Stolbovoi V., and I. McCallum. CD-ROM Land Resources of Russia. International Institute for Applied Systems Analysis and the Russian Academy of Science, Laxenburg, Austria

Olson, D.M., Dinerstein, E., Wikramanayake, E.D., Burgess, N.D., Powell G.V.N. and others, 2001, Terrestrial ecoregions of the World: A new map of life on Earth. *BioScience*, 51 (11), 933-938.

Paithoonwattanakij, K., 1989, Automatic pattern recognition techniques for geothermal correction on satellite data. PhD thesis, Dundee University.

Pauley, E.F., Nodvin, S.C., Nicholas, N.S., Rose, A.K. and Coffey, T.B., 1996, Vegetation, biomass, and nitrogen pools in a spruce-fir forest of the Great Smoky Mountains National Park. *Bulletin of the Torrey Botanical Club*, 123 (4), 318-329.

Rempel, R., 2006, Patch Analyst 3. Available online at: http://flash.lakeheadu.ca/~rrempel/patch/ (accessed 14 May 2007)

Röser, C., Montagnani, L., Schulze, E.-D., Mollicone, D., Kolle, O. and others, 2002, Net CO2 exchange rates in three different successional stages of the "Dark Taiga" of central Siberia. *Tellus*, 54B, 642-654.

Schiermeier, Q., 2005, Climate change: That sinking feeling. *Nature*, 435, 732-733.

Schulze, E.-D., Lloyd, J., Kelliher, F.M., Wirth, C., Rebmann, C. and others, 1999, Productivity of forests in the Eurosiberian boreal region and their potential to act as a carbon sink – a synthesis. *Global Change Biology*, 5, 703-722.

Shugart, H.H., Michaels, P.J., Smith, T.M., Weinstein, D.A. and Rastetter, E.B., 1988, Simulation Models of Forest Succession. In *Scales and Global Change - spatial and temporal variability in biospheric and geospheric processes*, T. Rosswall, R.G. Woodmansee and P.G. Risser (Eds.) (New York: Chichester [West Sussex]), pp. 125-151.

Shvidenko, A.Z., Nilsson, S., Stolbovoi, V.S., Gluck, M., Shchepashchenko, D.G. and Rozhkov, V.A., 2000, Aggregated estimation of the basic parameters of biological production and the carbon budget of Russian terrestrial ecosystems: 1. Stocks of plant organic mass. *Russian Journal of Ecology*, 31 (6), 371-378.

Smith, L.C., MacDonald, G.M., Velichko, A.A., Beilman, D.W., Borisova, O.K., and others, 2004, Siberian peatlands: A net carbon sink and global methane source since the early Holocene. *Science*, 303, 353-356.

Soja, A.J., Sukhinin, A.I., Cahoon, D.R., Shugart, H.H. and Stackhouse, P.W., 2004, AVHRR-derived fire frequency, distribution and area burned in Siberia. *International Journal of Remote Sensing*, 25(10), 1939-1960.

Sokolova, N., 2000, Institutions and the Emergence of Markets: Transition in the Krasnoyarsk Forest Sector, IR-00-028, IIASA, Laxenburg, Austria, 76 pp.

Strahler, A.H., Woodcock, C.E. and Smith, J.A., 1986, On the nature of models in remote sensing. *Remote Sensing of Environment*, 20, 121-139.

Sukhinin, A.I., French, N.H.F., Kasischke, E.S., Hewson, J.H., Soja, A.J. and others, 2004, AVHRR-based mapping of fires in Russia: New products for fire management and carbon cycle studies. *Remote Sensing of Environment*, 93, 546-564.

Townshend, J.R.G., 1981, Spatial resolution of satellite images. *Progress in Physical Geography*, 5, 33-55.

Turner, D.P., Cohen, W.B. and Kennedy, R.E., 2000, Alternative spatial resolutions and estimation of carbon flux over a managed forest landscape in Western Oregon. *Landscape Ecology*, 15, 441-452.

Vedrova, E.F., Shugalei, L.S. and Stakanov, V.D., 2002, The carbon balance in natural and disturbed forests of the southern taiga in central Siberia. *Journal of Vegetation Science*, 13, 341-350.

Wagner, W., Luckman, A., Vietmeier, J., Tansey, K., Balzter, H. and others, 2003, Large-scale mapping of boreal forest in SIBERIA using ERS tandem coherence and JERS backscatter data. *Remote Sensing of Environment*, 85, 125-144.

World Meteorological Organization, 2007, World Weather Information Service. Available online at: http://www.worldweather.org/107/m107.htm (accessed 4 March 2007)

Yan, X. and Shugart, H.H., 2005, FAREAST: A forest gap model to simulate dynamics and patterns of eastern Eurasian forests. *Journal of Biogeography*, 32, 1641-1658.

Zhang, Y.-H., Wooster, M.J., Tutubalina, O. and Perry, G.L.W., 2003, Monthly burned area and forest fire carbon emission estimates for the Russian Federation from SPOT VGT. *Remote Sensing of Environment*, 87, 1-15.

Chapter V

Summary

Trends of primary production along an urban-rural gradient in Southeastern Michigan and changes in forest biomass in three sample sites in Taiga ecoregions of Eastern Siberia were examined using remote sensing techniques and ecosystem models. Results showed that both regions had experienced abandonment of agriculture and increase in proportions of woody species (tree-cover expansion in Southeastern Michigan and forest regrowth in Eastern Siberia), and that, on average, the total annual CO_2 uptake increased by 53 g C m^{-2} in Southeastern Michigan and aboveground carbon storage in vegetation increased by 3.9 Mg C ha^{-1} (equivalent to 390 g C m^{-2}) in Eastern Siberia during the 1990s. This implies that both of these study areas have experienced increasing vegetation photosynthesis activities over the last decade of twentieth century.

Increases in northern hemisphere vegetation activity in the 1990s have also been documented in other previous studies (e.g., Keeling *et al.*, 1996). NDVI was found to increase significantly in the two study areas of my research between 1991 and 1999 (Slayback *et al.*, 2003), indicating the potential capability of terrestrial vegetation in absorbing atmospheric CO_2 in these regions. Atmospheric inversion models showed that the northern hemisphere land is a significant carbon sink, absorbing 1.53-2.89 Pg C yr^{-1} during the 1990s (Baker, 2007). The forest area is 8.21×10^8 ha in Russia (Houghton, 2005), and biomass increased 3.9 Mg C ha^{-1} from 1990 to 2000 (Chapter IV). Assuming

that our sample sites in Eastern Siberia represent the average biomass changes of the Russian forests, the aboveground vegetation in boreal and temperate forests in Russia can be estimated to have absorbed 3.2 Pg C between 1990 and 2000 due to land-cover dynamics alone. This is 43% of the total biomass increment estimated in vegetation and soils of Russian forests during 1981-1999 (Beer *et al.*, 2006). The annual net carbon uptake by Russian forests, which can be estimated to be 0.32 Pg C yr^{-1} in 1990s based on our results between 1990 and 2000 (i.e., 3.2 Pg C divided by 10 years), contributes to up to 21% of the annual net uptake of the entire northern hemisphere land (Baker, 2007). This number is comparable to the earlier research findings, which showed that Russian forests absorbed 0.28 Pg C yr^{-1} between 1995 and 1999 (Dong *et al.*, 2003). It is about half of the size of carbon sinks throughout North America and Eurasia and is 2.5 times of the net uptake by tropical land (Dong *et al.*, 2003; Baker, 2007), indicating that vegetation in Russian forests played an important role in fixing the atmospheric CO_2 in the 1990s.

The impacts of human development on carbon uptake from the atmosphere, not considering losses to respiration, were shown to vary by development densities according to the Michigan case study (Chapter II). The high level of GPP in exurban areas of Southeastern Michigan (about 1,992 g C m^{-2} yr^{-1} in 1991, which was higher than GPP in rural areas by 62 g C m^{-2} yr^{-1}) is consistent with previous research findings that, during the growing season, peri-urban areas were more productive than non-urban areas by approximately 70 g C m^{-2} yr^{-1} in the U.S. Midwest in 1992-1993 (Imhoff *et al.*, 2004). The estimated annual GPP was comparable to the estimation over the same region drawn from the global GPP/NPP product (Heinsch *et al.*, 2003), with the root mean squared

error of 145 g C m^{-1} $year^{-1}$ (less than 5% of the maximum pixel-wise GPP in 1999). The annual GPP in exurban areas (1,992 g C m^{-2} yr^{-1} in 1991 and 2,128 g C m^{-1} yr^{-1} in 1999) is much higher than the average global land GPP (877 ± 165 g C m^{-2} yr^{-1}; Cramer *et al.*, 1999) or average GPP values of the global temperate grasslands and crops (456 and 890 g C m^{-2} yr^{-1}, respectively; Prince and Gower 1995, Zheng *et al.* 2003, Zhao *et al.* 2005). This indicates that land conversion and landscaping strategies may help low-density development exurban areas maintain high vegetation productivity.

Previous studies also indicated that there is regional heterogeneity in the effects of urbanization and exurbanization. Urban sprawl resulted in increases of vegetation greenness in some U.S. cities (e.g., Denver, CO, where open shrublands in the urbanized area were greener than those in urban outskirt; Imhoff *et al.*, 2000) while it reduced net primary production in other U.S. cities (e.g., cities in the Southeastern U.S. contributed to 0.4% decline of the regional net primary production; Milesi *et al.* 2003). In Chapter II, exurban areas in Southeastern Michigan were found to associate with enhanced increase of GPP, which contradicts both of the above findings. This may occur due to regional differences in the response of ecological productivity to urban sprawl; or, alternatively, it may result from different approaches in defining development types. Development categories were determined based on Census housing density for the Michigan case study, while they were classified based on satellite images for the two comparison studies. Exurban, typically low-density development (10-40 acre per housing unit), may appear to be the "non-urban" category in maps based on imagery classification.

For both study cases, uncertainties in the carbon estimates relating to spatial scales were evaluated. For the Michigan case, I investigated the problem of scale

dependence in spatial units used to summarize productivity observations based on remote sensing images and related them to Census data on housing unit density. Spatial scaling of Census aggregation units was not found to affect inferences about productivity trends across settlement development types. This implies the feasibility of using coarse-scale Census data in detecting the impacts of human-housing development on ecosystem carbon functions at the nation level. For the Siberian case, effects of changes in observation scale (i.e., remote sensing image resolution) on the estimated changes in forest aboveground standing biomass were examined. Estimates of biomass changes were found to change with sensor resolutions due to the patch characteristics of disturbance and regrowth events that vary by a wide range in sizes. Accordingly, this overestimation of biomass accumulation or loss may have consequences for the global carbon accounting, which is often based on coarse-resolution remote sensing data. The scaling studies showed that inferences about carbon trends based on spatial data are influenced by scales of analysis, though scale dependence may vary depending on the nature of variables under analysis.

My research on evaluating carbon trends in the two representative landscapes contributes to the understanding of human and natural disturbance impacts on ecosystem carbon functions at the local to regional scales. The growth of human settlement has been rapid in the mid-latitude northern hemisphere, but their impacts on carbon dynamics are not fully understood. Human activities may be reduced in remote places such as Eastern Siberia; however, they are still present and occur repeatedly. Their impacts on the carbon cycle, together with those from the repeated natural disturbances, are difficult to evaluate due to the limited accessibility in these remote areas. Research methods of incorporating

remotely sensed land-cover and biophysical data and other ancillary data (such as climate records, Census data, and ecosystem model outputs) provide a promising approach for carbon accounting under multiple human and natural disturbance regimes over the large geographic extents. However, results also showed that the scale of analysis matters in the interpretation of carbon trends; therefore, appropriately determining scale of observation and scale of inference may be critical for estimation of carbon changes.

Extending from the present research, new projects may be developed in two directions. The first is to apply the approaches and knowledge gained here to account for changes in productivity and biomass across broader geographic extents. The second is to research the full path of carbon sequestration (e.g., from GPP to net primary production, NPP, and to net ecosystem production, NEP) in urban and ecological systems at northern hemisphere mid-latitude. The second research direction requires new developments in ecosystem modeling that take into account respiration of plants and higher-level consumers, while the first research direction is a more straightforward extension from the present research. Corresponding to the geographic locations in current studies, the immediate future projects may be evaluating productivity trends under urbanization across the entire U.S. and assessing biomass changes over the entire Eastern Siberia.

5.1 ΔGPP due to development across the U.S.

A future project might seek to understand human settlement impacts on changes in primary production. In the study of Southeastern Michigan, low-density development in the exurban area was shown to increase GPP, rather than reducing it, due to the increasing proportion of tree cover by converting agricultural lands to tree-dominated human settlement. Similar trends have been documented in the U.S. Midwest (Imhoff *et*

al. 2004). However, opposite trends were found in the southeastern U.S. (Milesi *et al.* 2003). The contradictory results indicate spatial heterogeneity of development effects on ecosystem carbon functioning. By investigating GPP trends and their relationships to land-cover changes in a systematic way across the U.S., we will have a better idea on where and why the carbon sources and sinks occur due to development land conversions.

My research demonstrated how ΔGPP can be estimated using AVHRR NDVI, solar radiation, and land-cover data. The biweekly NDVI composites are available across the entire U.S. from 1989 to present. The monthly mean surface solar irradiance data are available for the U.S. from 1983 to 1991 and after 1996. The U.S. land-cover data at 30-meter spatial resolution are publicly available based on classification of Landsat images acquired in 1992 and 2001. Given the satellite data availability, ΔGPP across the U.S. territory can be estimated between 1992 and 2001, using algorithm adopted in the current research.

Although the productivity trends across the U.S. can be summarized at any Census aggregation level, the Census-subdivision scale seems especially promising. At this scale, Census boundaries are relatively stable between 1990 and 2000, and, based on results in Chapter III, inferences about relationships between ΔGPP and development densities were generally equivalent to inferences drawn at the block-group scale. Census housing-unit data across the entire U.S. are available through websites of the U.S. Census Bureau. These data can be used to categorize all county subdivisions into different development types as used in the present study.

5.2 Biomass trends in Eastern Siberia

To calculate biomass changes at the landscape level, land-cover data based on Landsat imagery were combined with biomass values derived from ecosystem modeling. Theoretically, I believe this approach, with a few modifications, can also be applied to analyzing biomass changes in all of Eastern Siberia. In practical application, however, regional-scale estimation is difficult, because it is hard to obtain complete datasets of forest and disturbance types based on Landsat imagery given the data availability due to frequent cloud cover (Landsat has a 16-day repeating cycle; compared to MODIS/AVHRR with one-day repeating cycle, chance of obtaining cloud-free data drops to 1/16). An alternative option is to use the publicly available regional or global land-cover datasets to interpret forest, disturbances and other land-cover classes across the entire region. Previous research showed that AVHRR data collected at the 1.1-km spatial resolution is adequate for the classification of general forest types (e.g., dark-needled conifer vs. hardwood) in Siberia (Kharuk *et al.* 2003). This indicates that the global land-cover datasets based on AVHRR and MODIS data (Stralher *et al.* 1999, Hansen *et al.* 2000) can be used to derive the broadly defined land-cover types such as forests, wetland, agriculture and bare land (including cut). Historical disturbances such as fire and insect damage may be derived from previously published regional disturbance database (e.g., Kharuk *et al.* 2004, Sukhinin *et al.* 2004, George *et al.* 2006).

As discussed earlier, estimates based on the coarse-resolution remote sensing data are prone to bias because of the missing spatial details. Our analysis at the three sampled study sites suggested that missing disturbances caused up to 10% overestimate of biomass increment and that over represented large fires produced a 70% overestimate of

biomass loss. To characterize errors across the entire region, additional reference sites need to be established, which can make use of Landsat images, forest inventory data (Krankina *et al.* 2005), and/or radar-based wood volume products (Santoro *et al.* 2007).

References

Baker, D.F., 2007, Reassessing carbon sinks. *Science* 316 (5832): 1708-1709.

Beer, C., Lucht, W., Schmullius, C. and Shvidenko, A, 2006, Small net carbon dioxide uptake by Russian forests during 1981-1999. Geophysical Research Letters 33 (15): Art. No. L15403 Aug 4 2006.

Cramer, W., Kicklighter, D.W., Bondeau, A., Moore III, B., Churkina, G. and others, 1999, Comparing global models of terrestrial net primary productivity (NPP): overview and key results. *Global Change Biology* 5 (suppl. 1): 1-15.

George, C., Rowland, C., Gerard, F. and Balzter, H., 2006, Retrospective mapping of burnt areas in Central Siberia using a modification of the normalized difference water index. *Remote Sensing of Environment* 104: 346-359.

Dong, J., Kaufmann, R.K., Myneni, R.B., Tucker, C.J., Kauppi, P.E. and other, Remote sensing estimates of boreal and temperate forest woody biomass: Carbon pools, sources, and sinks. *Remote Sensing of Environment* 84: 393-410.

Hansen, M., DeFries, R., Townshend, J.R.G. and Sohlberg, R., 2000, Global land cover classification at 1km resolution using a decision tree classifier. *International Journal of Remote Sensing* 21: 1331-1365.

Heinsch, F.A., Reeves, M, Votava, P, Kang, S., Melesi, C. and others, 2003, User's Guide: GPP and NPP (MOD17A2/A3) Products (NASA MODIS Land Algorithm). http://www.ntsg.umt.edu/modis/MOD17UsersGuide.pdf (last access 04 September 2007).

Houghton, R.A., 2005, Aboveground forest biomass and the global carbon balance. *Global Change Biology* 11: 945-958.

Imhoff, M.L., Tucker, C.J., Lawrence, W.T. and Stutzer, D.C., 2000, The use of multisource satellite and geospatial data to study the effect of urbanization on primay productivity in the United States. *IEEE Transactions on Geoscience and Remote Sensing* 38 (6): 2549-2556.

Imhoff, M.L., Bounoua, L., DeFries, R., Lawrence, W.T., Stutzer, D., Tucker, C.J. and Ricketts, T., 2004, The consequences of urban land transformation on net primary productivity in the United States. *Remote Sensing of Environment* 89: 434-443.

Keeling, C.D., Chi, J.F.S. and Whorf, T.P., 1996, Increased activity of northern vegetation inferred from atmospheric CO_2 measurements. *Nature* 382 (6587): 146-149.

Kharuk, V.I., Ranson, K.J., Burenina, T.A. and Fedotova, E.V., 2003, Mapping of Siberian forest landscapes along the Yenisey transact with AVHRR. *International Journal of Remote Sensing* 24 (1): 23-37.

Kharuk, V.I., Ranson, K.J., Kozuhovskaya, A.G., Kondakov, Y.P. and Pestunov, I.A., 2004, NOAA/AVHRR satellite detection of Siberian silkmoth outbreaks in eastern Siberia. *International Journal of Remote Sensing* 25 (24): 5543-5555.

Krankina, O.N., Houghton, R.A., Harmon, M.E., Hogg, E.H., Butman, H.D. and others, 2005, Effects of climate, disturbance, and species on forest biomass across Russia. *Canadian Journal of Forest Research* 35: 2281-2293.

Milesi, C., Elvidge, C.D., Nemani, R.R. and Running, S.W., 2003, Assessing the impact of urban land development on net primary productivity in the southeastern United States. *Remote Sensing of Environment* 86: 401-410.

Prince, S.D. and Gower, S.N., 1995, Global primary production: A remote sensing approach. *Journal of Biogeography* 22: 815-835.

Santoro, M., Shvidenko, A., McCallum, I., Askne, J. and Schmullius, C., 2007, Properties of ERS-1/2 coherence in the Siberian boreal forest and implications for stem volume retrieval. *Remote Sensing of Environment* 106: 154-172.

Slayback, D.A., Pinzon, J.E., Los, S.O. and Tucker, C.J., 2003, Northern hemisphere photosynthetic trends 1982-99. *Global Change Biology* 9 (1): 1-15.

Strahler, A., Muchoney, D., Borak, J., Friedl, M., Gopal, S. and others, 1999, MODIS Land Cover and Land-Cover Change, MODIS Land Cover Product Algorithm Theoretical Basis Document (ATBD, version 5.0). Available online at: http://modis.gsfc.nasa.gov/data/atbd/atbd_mod12.pdf (last access 12 March 2007)

Sukhinin, A.I., French, N.H.F., Kasischke, E.S., Hewson, J.H., Soja, A.J. and others, 2004, AVHRR-based mapping of fires in Russia: New products for fire management and carbon cycle studies. *Remote Sensing of Environment* 93: 546-564.

Zheng, D., Prince, S. and Wright, R., Terrestrial net primary production estimates for 0.5° grid cells from field observations – a contribution to global biogeochemical modeling. *Global Change Biology* 9: 46-64.

Zhao, M., Heinsch, F.A., Nemani, R.R. and Running, S.W., 2005, Improvements of the MODIS terrestrial gross and net primary production global data set. *Remote Sensing of Environment* 95: 164–176.